THE FAILURE OF TETON DAM – A NEW THEORY BASED ON "STATE BASED SOIL MECHANICS"

By

NAVARATNARAJAH SASIHARAN

A thesis submitted in partial fulfillment of
the requirements for the degree of

MASTER OF SCIENCE IN CIVIL ENGINEERING

WASHINGTON STATE UNIVERSITY
Department of Civil and Environmental Engineering

December 2003

To the Faculty of Washington State University:

The members of the Committee appointed to examine the thesis of NAVARATNARAJAH SASIHARAN find it satisfactory and recommend that it be accepted.

_____

Chair

_____

_____

ACKNOWLEDGEMENT

First of all, I would like to express my great appreciation to Dr.Balasingam Muhunthan for his irreplaceable encouragement, guidance and support throughout this study. He has been an inspiration to me since I applied for admission to Washington State University. A person of myriad skills, he has eased the way of my work by his wonderful contribution. He volunteered many hours of his valuable time to help me put my best foot forward.

I would also like to express my thanks to Mr. V.S Pillai, Geotechnical Engineer, Vancouver, B.C, for being a veritable wellspring of ideas and suggestions pertaining to this research. His vast knowledge on dam construction and experience made this project possible and even more enjoyable. Also, I wish to thank Dr. Adrian Rodriguez-Marek and Dr. William Cofer for their assistance in this study. My gratitude also goes to my colleagues in GeoTransportation group, especially Mr. Omar Al-Hattamleh and Sathish Balamuragan for helping me in many ways.

Financial support by the National Science Foundation (Grant CMS-0234130) and Washington State Department of Transportation is acknowledged with gratitude.

Last but certainly not least, I would like to express my deepest gratitude for the constant support, understanding and love that I received from my wife Lojini and my family during the this study.

THE FAILURE OF TETON DAM – A NEW THEORY BASED

ON "STATE BASED SOIL MECHANICS"

Abstract

by Navaratnarajah Sasiharan, M.S.
Washington State University
December 2003

Chair: Balasingam Muhunthan

Teton Dam failed during its first filling on 5 June 1976. The 405-ft high dam was designed and built using modern standards; therefore its failure received considerable scrutiny from engineering experts. Failure mechanisms suggested included hydraulic fracture, internal erosion, wet-seam theory, and defects in the abutment rock. None of the investigations, however, were able to explain satisfactorily why the dam breached when the reservoir reached EL.5301.7 ft and only in the vicinity of Sta. 14+00 on the right abutment. The investigation here is focused on this crucial aspect of the failure using the modern framework of fundamental "state based soil mechanics". According to this framework, highly compacted soils of low plasticity in an environment of low liquidity index and low confining stress would crack in the presence of high shear stresses. The impervious core (Zone-1) of Teton was constructed with highly compacted uniform clayey silt of low plasticity and therefore was prone to such a possibility. This thesis describes the details of the theory, the investigation, and the conclusions arrived at regarding the potential initiation of Teton failure. Furthermore, it critically evaluates the

failure mechanisms proposed by previous investigations based on the results obtained and the framework of state based soil mechanics.

Finite element analysis carried out using state based parameters indicate the presence of deep open transverse vertical crack(s) in the core (Zone-1) to a maximum depth of about 32 ft from the crest only in the right abutment and in the vicinity of Sta. 14+00. It is concluded that once the water level in the reservoir rose above El 5300.0 ft in the early hours of 5 June 1976 water flowed through the open vertical crack(s), which slowly eroded the crack into a large tunnel leading to the major breach of the dam hours later.

TABLE OF CONTENTS

Page

Page

Page

LIST OF TABLES

Page

LIST OF FIGURES

Page

Page

CHAPTER ONE

INTRODUCTION

1.1 Teton dam failure

The 405-ft high Teton dam that was built in Idaho failed during its first filling on June 5, 1976. Its failure was one of the most publicized events involving a large earth fill dam in recent history. Its failure resulted in 14 fatalities and an economic loss in excess of $400 million at that time. Teton dam was designed and built using modern standards (Muhunthan and Schofield, 2000). Therefore, its failure received the most attention from engineering experts around the world. However, the failure assessment and prognosis by experts including those by the Independent Panel (IP, 1976) and the Interior Review Group (IRG, 1980) failed to arrive at a consensus. The failure mechanisms suggested included hydraulic fracture, internal erosion, the wet-seam theory, defect in the abutment rock, etc. (Seed et al.1976; Leonards, 1986). The conclusions were generic and less convincing. None of these investigations provided any concrete evidence as to why the dam breached when the reservoir level reached EL.5300.7 ft and only at around Sta.14+00 on the right abutment. Therefore, a full understanding of the mechanism of this key aspect of failure may make an important contribution to the state-of-the-art for dam construction.

The impervious core/water barrier (Zone-1) of Teton was constructed of uniform clayey silt of low plasticity and low liquidity index. Highly compacted soils of low plasticity tend to crack in an environment of low liquidity index, low confining stresses and high shear stresses (Muhunthan and Schofield, 2000). None of the previous investigations focused on the possibility of the presence of cracks in the upper portions of

the dam. Such a possibility is investigated here using the concepts of the framework of "state based soil mechanics" (Pillai and Muhunthan 2001, 2002).

The state based soil mechanics has its origins from the Critical State Soil Mechanics (CSSM) framework (Schofield and Wroth, 1968; Schofield, 1980; Muhunthan and Schofield, 2000). It is assumed that the mechanical behavior of soil such as compressibility, pore pressure response, shear behavior with respect to yield, rupture and fracture is dependent on the "state of soil" in q-p'-e (Shear stress-mean stress-void ratio) space or equivalently the LI-p' (Liquidity index-mean stress) space. The stress states that delineate yield, rupture, and fracture are defined for each soil material based on material properties. The state of soil in q-p'-e space can be determined analytically or using numerical methods such as the Finite Element, Finite difference methods, etc. in conjunction with the mechanical properties of the material obtained from laboratory tests. If the state of soil approaches the fracture surface, the soil tends to develop cracks. Similarly the state of soil in LI-p' space is determined from physical properties of the material such as the liquid limit and plastic limit. This provides two independent approaches to determine the state of a soil and determine its behavior regime.

Laboratory tests on Teton Zone-1 material are carried out to determine its physical and mechanical properties. Finite element analyses are conducted using widely used commercial finite element software package ABAQUS. The numerical results in combination with state based soil mechanics principles are used to identify the state of Teton Zone-1 compacted material. These results and LI and p' contour are used to identify the main cause of the Teton failure.

1.2 Research Focus

The primary objective of the research is to identify the main mechanism of the initiation of failure of Teton dam using state based fundamental soil mechanics. The problem is investigated by the two independent approaches as explained above. Finite element analyses are performed for the two-dimensional cross-section of the dam using appropriate material properties. From the results of the finite element analyses, the states of soil in terms of stress ratio (q/p') are computed for the Teton valley cross-section. The q/p' ratios are used to identify the zones of fracture (cracks), rupture and yield within the cross-valley section. This stress ratio approach is based on the mechanical properties of the soils.

Another independent approach using the physical properties of the soil is also explored. Contours of liquidity against effective mean pressure are plotted in the Liquidity-confining stress (LI- lnp') space. From these plots, zones of soil states that approach the "crack surface" (fracture) will be mapped on the cross sections to determine the depths of soils that are prone for cracking. The results of this method are compared with those based on the stress ratio and stress space.

1.3 Organization of Thesis

This thesis consists of seven chapters. Chapter 2 gives a detailed background of the theory and concepts that have been used in this research. The history of Teton dam construction and failure is given in Chapter 3. It describes the construction details and the events leading to the failure of Teton dam. The review includes a critical evaluation of the results of previous investigations carried out by the IP and the IRG. Chapter 4

presents details of the experimental program. Chapter 5 presents the details of the finite element analysis. It includes the description of the constitutive model, type of mesh, and boundary conditions employed in the study. Chapter 6 presents a detailed discussion of the results of the analyses. It also critically evaluates the previous failure mechanisms in light of the results obtained here. Chapter 7 presents the conclusions arrived based on the laboratory and finite element investigations. Proposal for refining the analyses as well as recommendation for the future dam construction guidelines are also provided.

CHAPTER TWO

CRITICAL STATE SOIL MECHANICS

2.1 Limiting State boundaries for sedimentary deposit

Figure 2-1 shows a sedimentary deposit of saturated remolded (isotropic and homogeneous) aggregates of grains with particles falling on to the surface and forming a deposit. As the deposit builds up the effective spherical pressure on any layer of material increases steadily. The deposit exhibits three distinct classes of behavior.

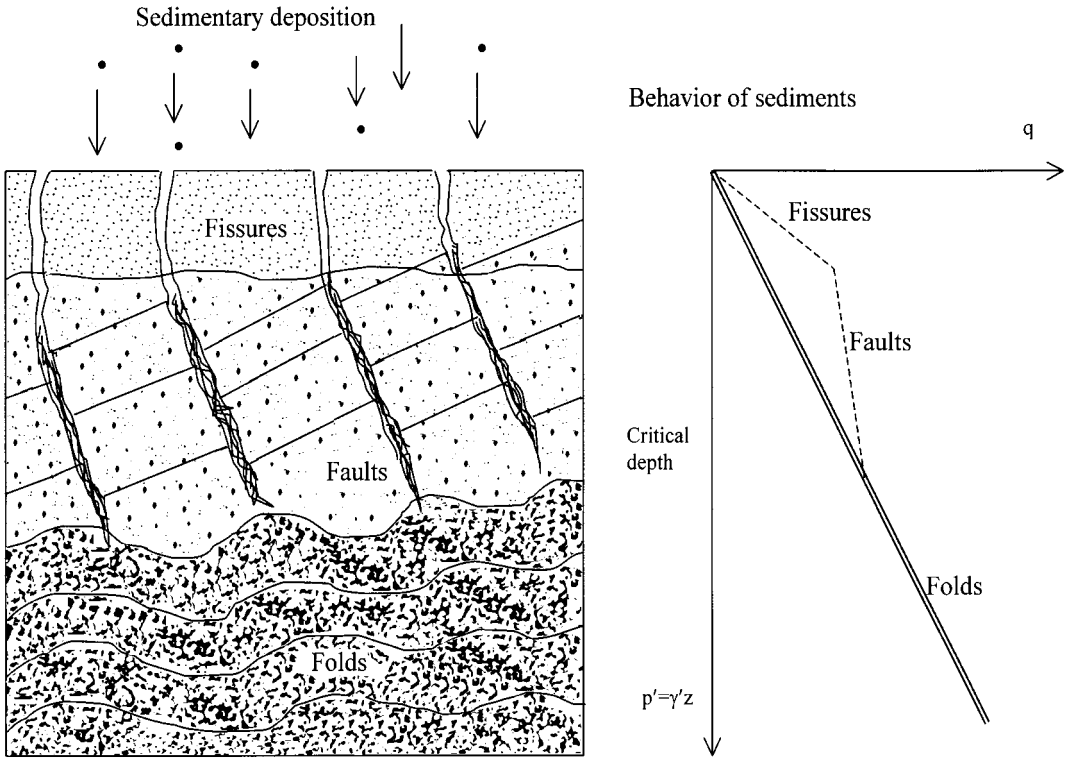

Figure 2-1: Sedimentary deposits and limiting state lines

At large depths, higher pressures cause ductile yielding of the aggregates and the layer of sediments to *fold*. Above these depths and at lower pressures, aggregates rupture and a layer of sediments *faults* with the presence of gouge material along the slip planes.

Near the surface where the pressure is nearly zero, a layer of sediment fractures or cracks and aggregates can disintegrate.

Critical state soil mechanics captures the above depositional and structural phenomena of folds, faults, and fractures in sedimentary as well as man-made deposits of soils in a scientific manner. It explicitly recognizes that soil is an aggregate of interlocking frictional particles and that the regimes of soil behavior depend in a major way on its density and effective pressure.

2.2 Soil behavior during shear deformation

All soils reach an ultimate state with continuous shearing at which they flow as a frictional fluid with no further changes in stress or volume. This ultimate state has been termed as critical state by the Cambridge group of researchers (Roscoe et al.1958). A unique relationship between the void ratio and the effective stresses at the critical state has also been observed by several researchers. They include observations on normally consolidated clay by Rendulic (1937) and on compacted clay by Leonards (1955) and on both normally and overconsolidated clay by Henkel (1960). The existence of a similar relationship for sands has been found by Ladanyi (1969).

Based on the observations of Rendulic, Leonards, and Henkel at the critical state, the Cambridge group of research put forward a comprehensive model for soil behavior. Many of the key critical state concepts, including the Cam-clay model of yielding for soils, had been set out in detail by Roscoe and Schofield (1963), Schofield and Togrol (1966), Schofield (1966), and in the textbook on critical state soil mechanics by Schofield and Wroth (1968). While original research efforts at Cambridge were concentrated on

clays, significant attention had also been given to sands (Thurairajah 1961; Wroth and Bassett 1965; Stroud 1971).

The family of Cam-clay models (Roscoe et al. 1963, Burland and Roscoe, 1968) has proven to be useful elasto-plastic models for soil behavior in finite element analysis.

2.3 Critical state and compression lines

The relationship between shear stress, effective confining pressure, and void ratio/specific volume can be represented as a unique critical state line in a three-dimensional q-p'-v space (Fig.2-2) (Roscoe et al. (1958)), where q is the deviator stress, p' is the mean normal stress and v is the specific volume. They are defined, respectively, as $p' = \frac{1}{3} I_1$, $q = \sqrt{3J_2}$, and, $v = 1 + e$, where:

$$I_1 = \frac{\sigma_1' + \sigma_2' + \sigma_3'}{3} \tag{2-1}$$

and

$$J_2 = \frac{1}{6}\left[(\sigma_1' - \sigma_2')^2 + (\sigma_2' - \sigma_3')^2 + (\sigma_3' - \sigma_1')^2\right] \tag{2-2}$$

with σ'_1, σ'_2 and σ'_3 being the principal stresses of a stress tensor and e being the void ratio. For triaxial conditions, where $\sigma'_2 = \sigma'_3$, the mean effective and deviatoric stresses reduce to:

$$p' = \frac{\sigma_1' + \sigma_2' + \sigma_3'}{3} \tag{2-3}$$

and

$$q = \sigma_1' - \sigma_3' \tag{2-4}$$

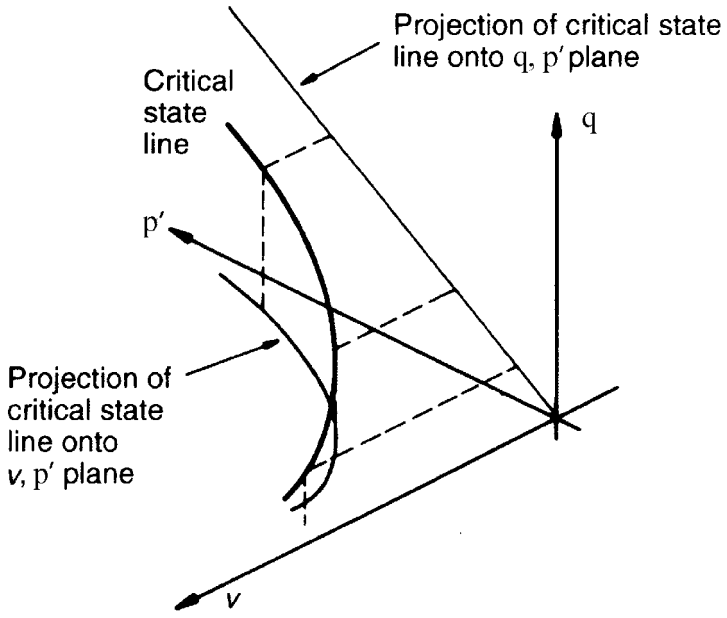

Figure 2-2: Critical state line in q- p'- v space

Projection of the critical state line (Fig.2-2) on q- p' space and v-lnp' space are given as:

$$q = Mp' \tag{2-5}$$

and

$$\Gamma = v + \lambda \ln p' \ , \tag{2-6}$$

respectively. M is the slope of critical state line in the p'- q space and Γ and λ are the intercept at p' = 1 kPa and slope of the critical state line in the v-lnp', respectively (Fig.2-3). Moreover, the critical state line is one of the families of parallel lines, which are different compression lines with equation $v_\lambda = v + \lambda \ln p'$. Note v_λ = Γ at the critical state.

Elastic compression and swelling lines are described by a general relationship in the v-lnp′ space given by the following:

$$v_\kappa = v + \kappa \ln p' \tag{2-7}$$

where v_κ is the intercept, and κ is the slope (Fig.2-3). The family of parallel elastic lines represents the amount of elastic volume change that occurs with changes in mean effective stress.

2.4 Aggregate behavior

The value of v_κ combines pressure p′ and specific volume v to define the aggregate of grains, which corresponds to the line through point A in Figure 2-3 (a). The elastic compression and swelling characteristics of the aggregate defines the slope of this line. The packing density of the aggregate of grains defines the intercept v_κ. For the ideal soil defined as Cam-clay there is no slip among the grains while the aggregate experiences purely elastic changes. Any slippage results in small plastic deformation of the aggregate as a whole, with changes of many contacts between grains. Each time there is plastic deformation a new aggregation of particles is formed, which has a swelling and compression line with the same slope but a different intercept. A shift between lines indicates a plastic volume change from one aggregation to the next. For illustrative purpose a plot of v_κ against ln p′ gives a clearer view of the shift of the lines (Fig.2-3 (b)). Note that the line of critical states in this plot has slope (λ - κ).

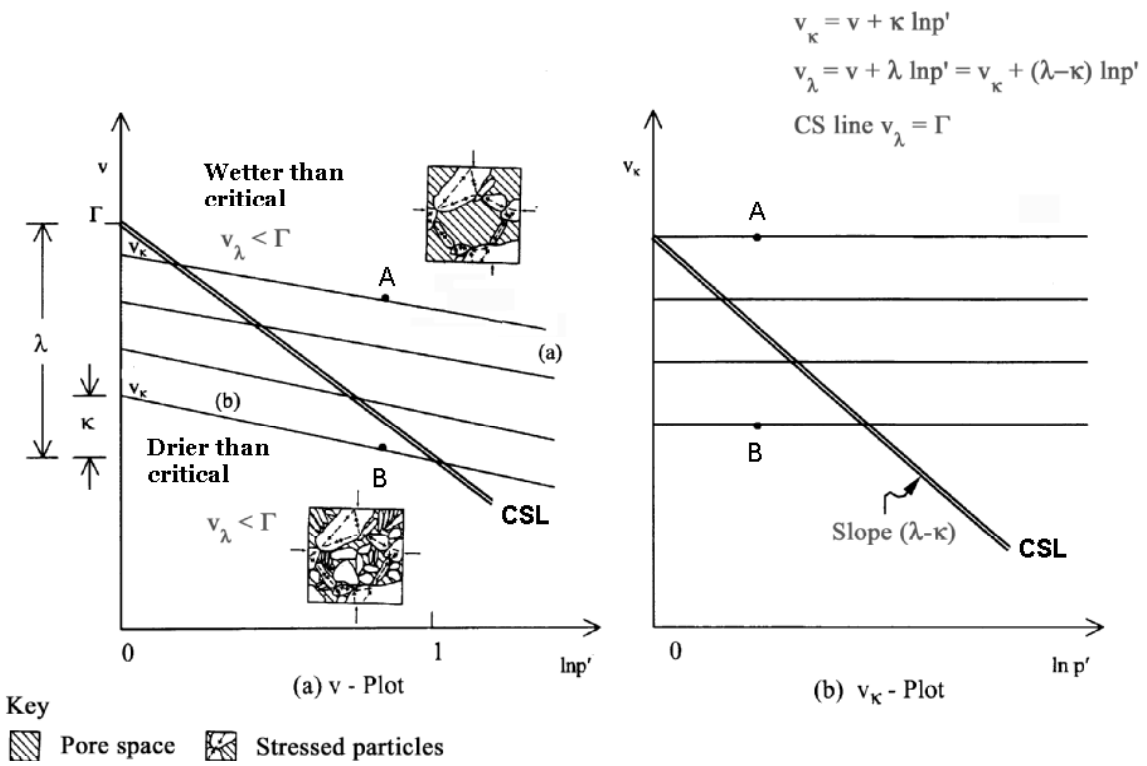

Figure 2-3: Aggregate behavior and critical states

(Muhunthan and Schofield, 2000)

Consider two specimens with aggregates of grains at the same mean normal effective stress on lines (A) and (B) with identical lattices of highly loaded grains, but with different amount of lightly loaded grains (Fig. 2-3(a)). If line (A) has a higher value of v_κ than line (B), then specimen (A) has fewer lightly loaded grains than specimen (B). If we now impose shear stresses on the aggregations represented by (A) and (B) and permit drainage of pore fluid, we may expect slippage of highly loaded particles and plastic volume change. This leads to other grains forming a highly loaded lattice.

The plastic volumetric response of the two specimens at the same mean effective stress will differ depending on the nature of packing of the lightly loaded grains. A

specimen on the line (A) with fewer lightly loaded grains loosely packed will compact with a fall in v_κ and the dense one on line (B) will dilate with increase in v_κ during plastic shear distortion. Between these two limits there will be a density of packing at which during shear distortion a succession of load carrying skeleton lattices of stressed grains will form and collapse with successive new structures being formed at about the same density of packing. In this shear strain increment a certain proportion of the grains which at one time formed the load carrying skeleton, now as individual grains become relatively lightly stressed or unstressed and play the role of "filler" particles filling voids. The notion of a critical state is that there exists one certain critical packing of grains or critical void ratio, at which continuous flow is possible at constant mean normal effective stress p', without damage to the grains, only with change of positions.

Recently a new insight into critical states links them with the angle of repose (Muhunthan & Schofield, 2000). In a loose drained heap of aggregate below a slope at an angle of repose there are elements of aggregate, which are at increasing pressure as their depth below the slope, increases (Fig.2-4). An element (i) has a certain value of v_κ. As successive layers of aggregate are added to the slope and (i) is buried below layers (ii) and (iii) this value of v_κ will increase as shown in Figure 2-4.

The critical state line can be used to distinguish two different classes of behavior of soils. There are states for which the combinations of specific volume v and mean normal effective stress p' lie further away from the origin than the line of critical states, so that,

$$v + \lambda \ln p' > \Gamma , \qquad \text{or} \qquad v_k + (\lambda - \kappa) \ln p' > \Gamma , \qquad \text{or} \qquad v_\lambda > \Gamma \qquad (2\text{–}8)$$

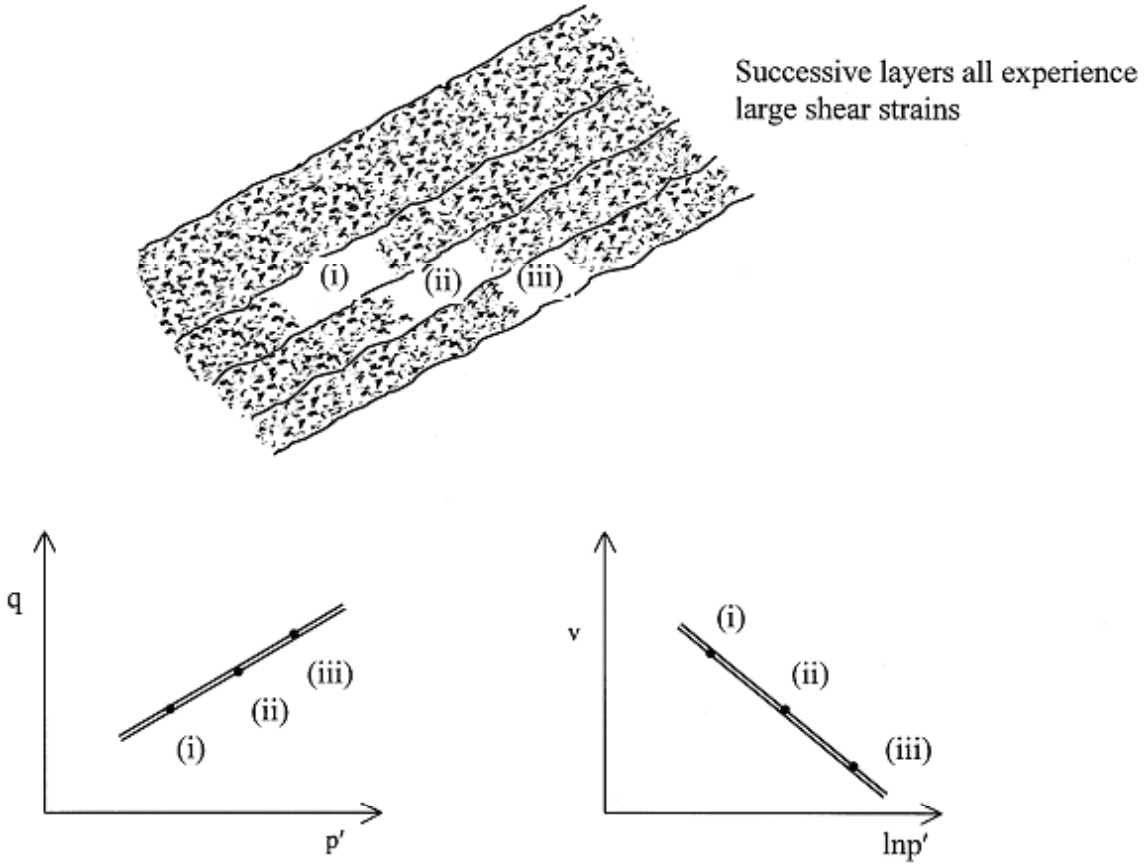

Figure 2-4: Slope at angle of repose and critical states.

and these states have been called “wetter than critical”; under such conditions shearing causes aggregates to compress to more dense packing and emit water with ductile stable yielding of a test specimen. There are also states of specific volume v and mean normal effective stress p′ such that

$$v + \lambda \ln p' < \Gamma , \qquad \text{or} \qquad v_k + (\lambda - \kappa) \ln p' < \Gamma , \quad \text{or} \qquad v_\lambda < \Gamma \qquad (2\text{-}9)$$

and these states have been called “drier than critical”; where shearing causes aggregates to dilate and suck in water and ground slips at peak strength with unstable failures.

2.5 Cam-clay model

At the core of CSSM was the creation of the constitutive model called Cam-clay. The Cam-clay theory combined the observations of the critical state and the theory of plasticity into a powerful model for prediction of the yielding of the specimen on the wet side of critical. The original Cam-clay model (Fig.2-5) was synthesized from two basic equations.

The first (Fig.2-5) shows that if yielding obeys the stable associated plastic flow rule then the product of the plastic flow increment (dv, dε) and any stress increment (dp′, dq) directed outward from the yield locus is positive or zero - the zero applies to stress increments directed along the tangent to the yield locus. This associated flow rule was deemed entirely appropriate to soil mechanics (Schofield 1980).

The second is an energy equation and explains that when yielding occurs the work is purely frictional and that the rate of dissipation during shear distortion is simply the product of p′ times the friction coefficient M. This was similar to the proposal by Taylor (1948). Thurairajah (1961) reported the analysis of drained and undrained triaxial test data, which confirmed the above energy equation.

After eliminating the dilatancy rate dv/dε between these two equations (Fig.2-5) a single differential equation is left which when integrated predicts the form of the cam-clay yield curve (CD in Fig. 2-5). The specimens on line CD have same v_κ and lie on one elastic compression and swelling line. Curve CD allows stress to extend a certain distance beyond the critical state line but there is a limit - when q = 0 the pressure cannot extend further than D, if the material is to remain stable. If there were soil in states

beyond D, it would be metastable. For example when salt is leached out of quick clay it gets into this dangerous state and there is a risk of a quick clay avalanche.

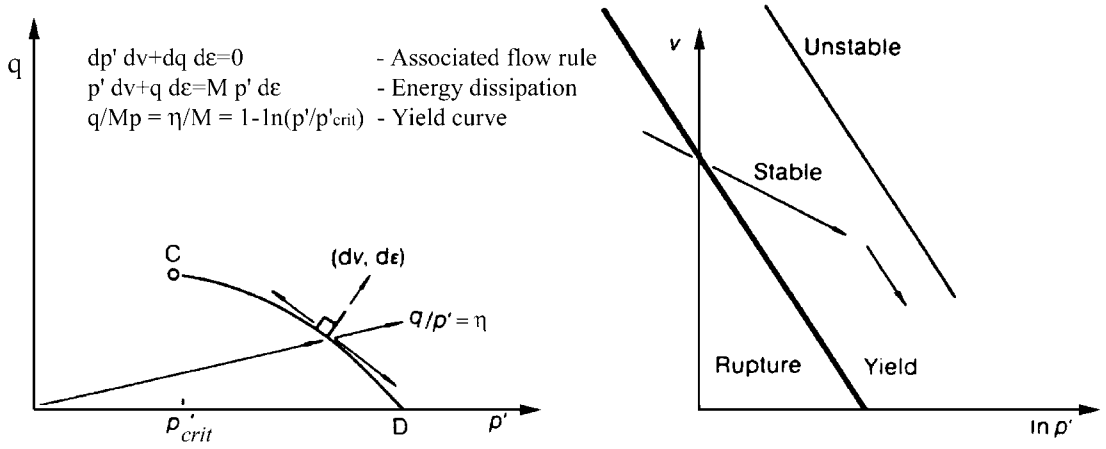

Figure 2-5: Cam-clay yielding (Schofield, 1980)

It was a strong outcome of the synthesis of the original Cam-clay model that it predicted an isotropic compression line with $v_\lambda = \Gamma + (\lambda - \kappa)$ that bounded the region of wet clay behaviour $\Gamma > v_\lambda > \Gamma + (\lambda - \kappa)$, exactly as was first observed by Casagrande and Albert (1930) and subsequently by Hvorslev (1937), Shibata (1963), and many others (Schofield, 1980).

2.6 Limiting states in q-p' stress space

Soil in a state drier than critical such as point F in Figure 2-6(b) has been observed to fail with well-defined rupture planes after reaching peak strength. This behavior is very familiar to geotechnical engineers. Based on a set of shear box data on Vienna clay obtained by his student Hvorslev (1937), Terzaghi interpreted these results in terms of a Mohr-Coulomb line with a slope termed “true friction” and a “true cohesion”

intercept (Fig.2-6 (a)). At MIT, Taylor (1948) interpreted sand shear box peak strength data in terms of interlocking and dilation. Interlocking clearly also contributes to the shear strength of clay. Schofield and Wroth (1968) re-examined Hvorslev's data in light of the Taylor's interlocking and found that the Terzaghi and Hvorslev failure line applied only for a restricted range of mean effective pressure and specific volume, and they attributed these peak strength data to critical state friction and interlocking. Therefore, it is appropriate to represent the Hvorslev's data as shown in Figure 2-6 (b) and the plane where the data fall was termed as the Hvorslev-Coulomb surface.

Limits to stable states of yielding in the critical state framework are defined by the state boundary surface in the 3-D, p-q-e space. The 2-D representations of the normalized state boundary surface in the q/p'_{crit} - p/p'_{crit} is shown in Figure 2-6 (c).

It has already been shown that the critical state line separates two different regimes of behavior. The region in which faulting is observed with dilation on gouge material is the region to which Mohr-Coulomb peak strength applies. Lines AB and GE (Fig.2-6 (c)) indicate Hvorslev's Coulomb faults on rupture planes. On the other side of the critical state line there is a regime in which soil does not bifurcate but yields and deforms as a continuum. The Cam-clay model describes the yielding behavior in states where layers can fold. Curves BD and ED indicate Cam-clay yield and fold of a sediment layer.

In states on the dry side the particles remain interlocked with each other and peak strength of soil involves a contribution from dilatancy of the interlocked stressed grains. The dilating gouge material on the rupture planes will slowly soften to critical state plane

strengths fitting lines OB and OE (Fig.2-6 (c)), although suction can persist for many years provided the soil aggregate does not fissure or crumble.

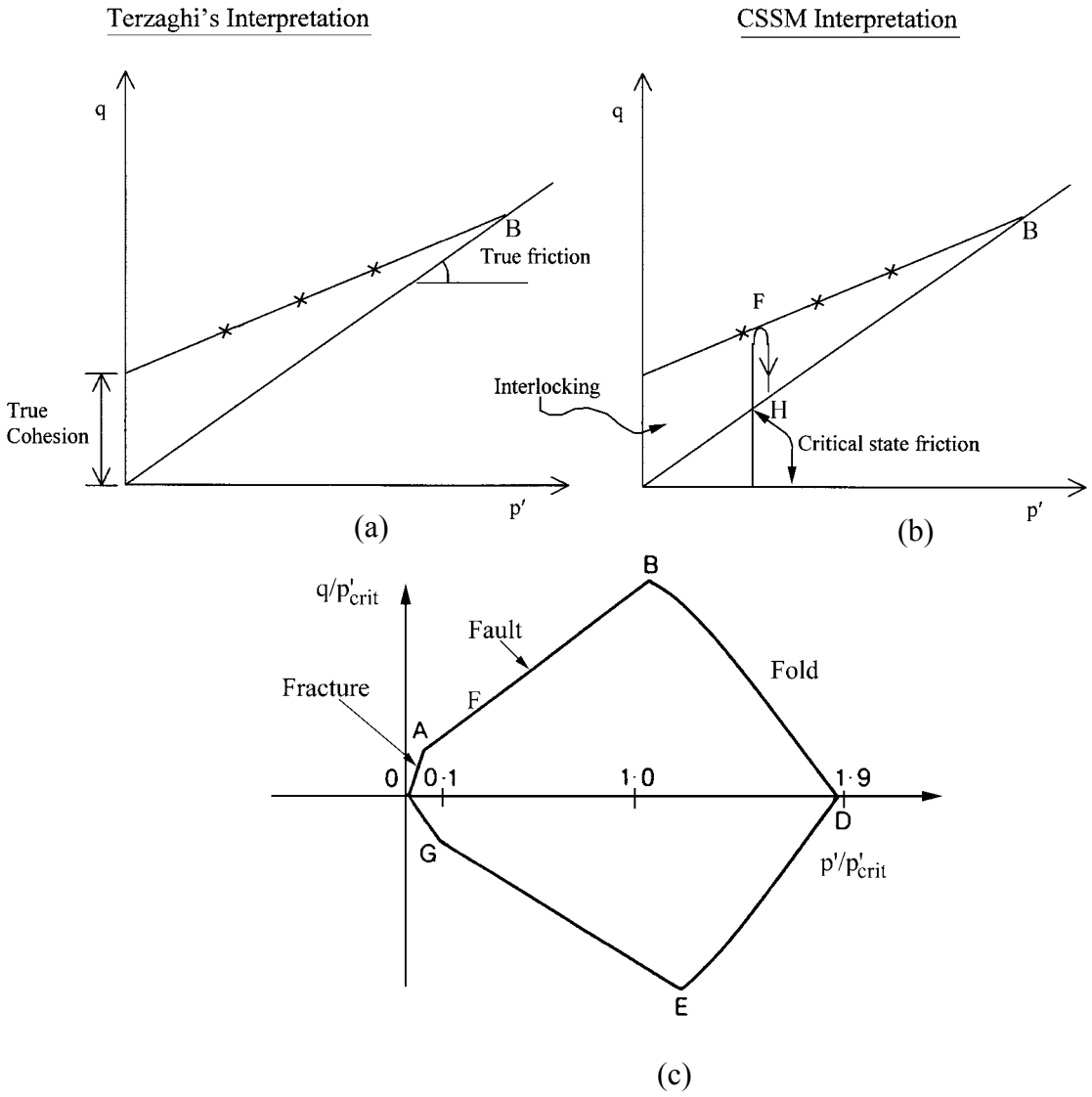

Figure 2-6: Schematic diagram of limits of stable states of soils in normalized q/p'_{crit} - p/p'_{cri} stress space (Muhunthan and Schofield, 2000)

Soil states on the crack surface result in the development of unstable fissures and crack openings. Heavily overconsolidated clays and overcompacted sands at low

confining stresses could reach this limiting state. Collapse similar to fracture on the dilative side can also exist on the contractive domain, but outside the normal consolidation line (Fig.2-7). Such states outside the stable yielding exist in wind deposited loose sands, air pluviated or moist-tamped sands and result abrupt collapse upon shearing of these materials (Pillai and Muhunthan, 2001, 2002). For sands and clayey silts of low plasticity, stable yield behavior occur only within a narrow band on both the looser and denser side of the critical state line (Fig.2-7).

The critical state line also forms a bound to the region of faulting. There is a broad region of states where faults can occur and this region is bounded at low mean effective pressure by soil cracks in tension. The "no tension" or "limiting tensile strain" criteria are the most widely used among the alternative theories to quantify tensile fracture (Schofield 1980). For the triaxial specimen the no tension criterion leads to $\sigma_a = 0$, which is the case of line OA, $p' = \sigma_a/3$, $q/p' = 3$, or to $\sigma_r = 0$ which is the case of line OG, $p' = 2/3\sigma_r$, $q = -\sigma_r$, $q/p' = -2/3$ (Fig.2-6 (c)). Based on Weald clay data, Schofield (1980) has suggested that the change to tensile fracture from Coulomb rupture occurs in the vicinity of $p'/p_{crit} = 0.1$, where p_c is the effective confining stress at critical state. This is equivalent an overconsolidation ratio of approximately 20 (Fig.2-6 (c)).

When the effective stress path crosses the crack surface OA, the soil element begins to disintegrate into a clastic body and unstressed grains become free to slide apart. In that case the average specific volume of the clastic mass can increase (large voids/cracks) and consequently its permeability can increase significantly and instantly. A significant internal/external shear stress at low confining stresses can cause the crossover of the crack-surface OA and a large increase in specific volume. When such

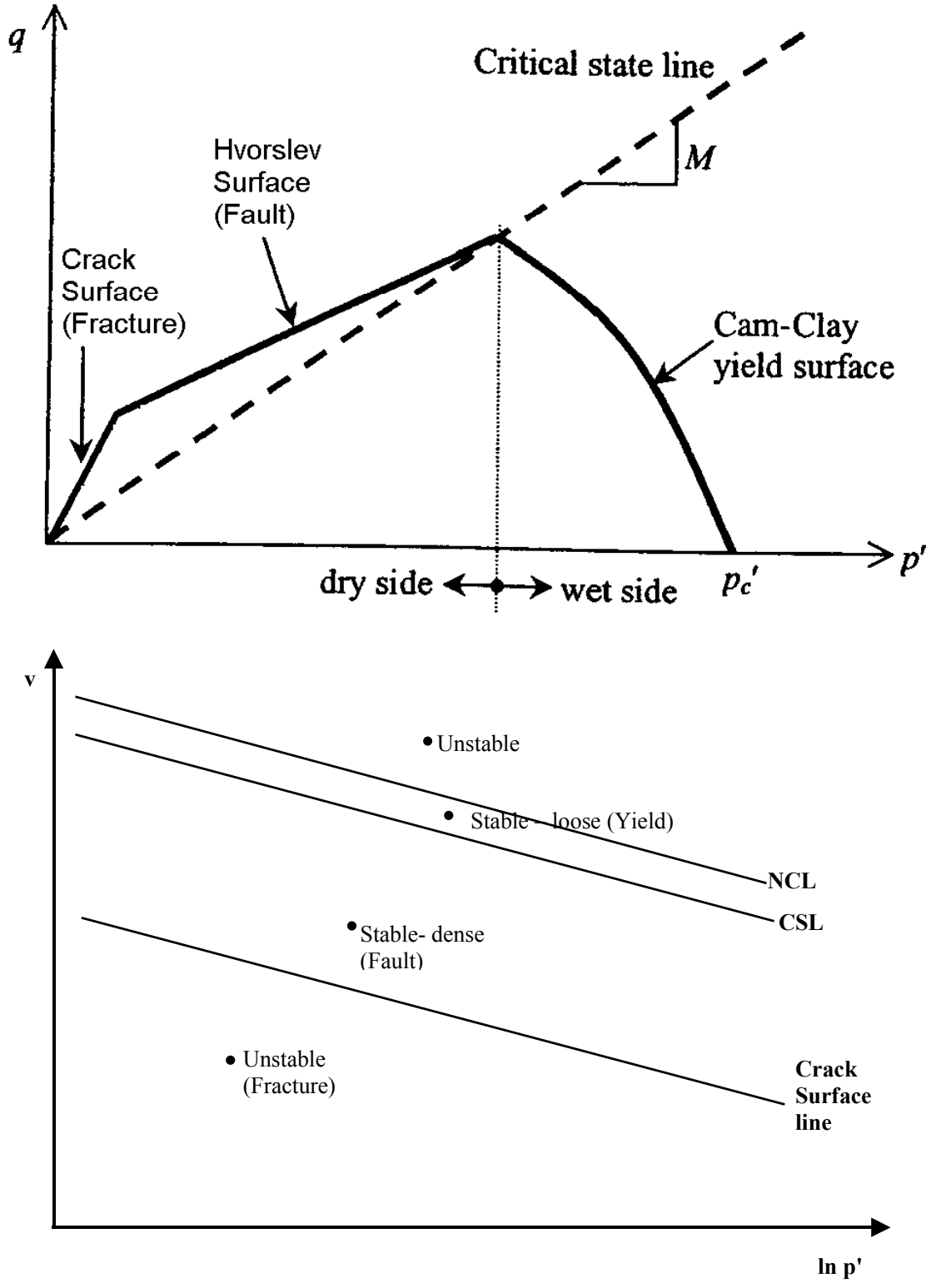

Figure 2-7: Limiting states of soil behavior in q-p' space and v-lnp' space

(Modified after Pillai and Muhunthan, 2002) (Schematic)

condition occurs, the opening within the soil body may be an extensive crack or a local pipe or channel. If such opening (crack/channel) day lights into the water body it could lead to a free flow of water into the downstream slope.

The characterization of soil as cohesive or frictional is not regarded in CSSM as a fixed property of a particular type of soil grain or mineral or pore fluid but rather depends on the state of stress and the specific volume of soil. In this view it is wrong to extrapolate the Mohr-Coulomb peak strength line to all ranges of pressure and specific volume. Further discussion on Terzaghi's Mohr-Coulomb error and its correction can be found in Schofield (1998).

The simple division of soil behaviour based on critical state theory at limiting states at one value of specific volume v shown in Figure 2-7 divides the behaviour at limiting states into three distinct classes of failure. The limiting lines OA and OG indicate states limited by *fractures or fissures*; AB and GE indicate that Hvorslev's Coulomb *faults* on rupture planes will limit behaviour; BD and ED indicate Cam-clay yield and sediment layer *folds*. The fractures, faults, and folds (FFF) diagram (Figure 2-1) is useful to characterize all classes of observed mechanisms of large displacements in soils. It is used here in the context of the characterization of the behavior of Teton Zone-1 material.

2.7 Critical state line in LI-lnp′ space

Figure 2-8 shows the family of experimental Critical State lines for different soils. It can be seen that if all the lines are extended they pass through a single point Ω given by $v_\Omega \approx 1.25$, $P_\Omega \approx 1500$ lb/in^2. Skempton and Northey (1953) showed that the strengths of

soils at the liquid limit and the plastic limit are constant and that the ratio of these strengths is 1:100. In addition, the effective spherical pressure at plastic limit (p_{PL}) was found to be approximately 80 lb/in^2 for all soils. The effective spherical pressures associated with liquid limits (p_{LL}) show a much wider range of values but this scatter is exaggerated by the logarithmic scale. Schofield and Wroth (1968) idealized these experimental observations (Fig. 2-9) with all lines passing through Ω, and p_{LL} and p_{PL} assumed to have fixed values.

Since the specific volume at the plastic limit and the liquid limit are known for each critical state line it is possible to convert the ordinate v to ordinate liquidity index (LI). Converting v ordinate to liquidity index (LI), all critical state lines fall into a unique straight line as shown in Figure 2-10. Critical state line of most soils coincides with the same unique critical state line once they have been normalized as explained above.

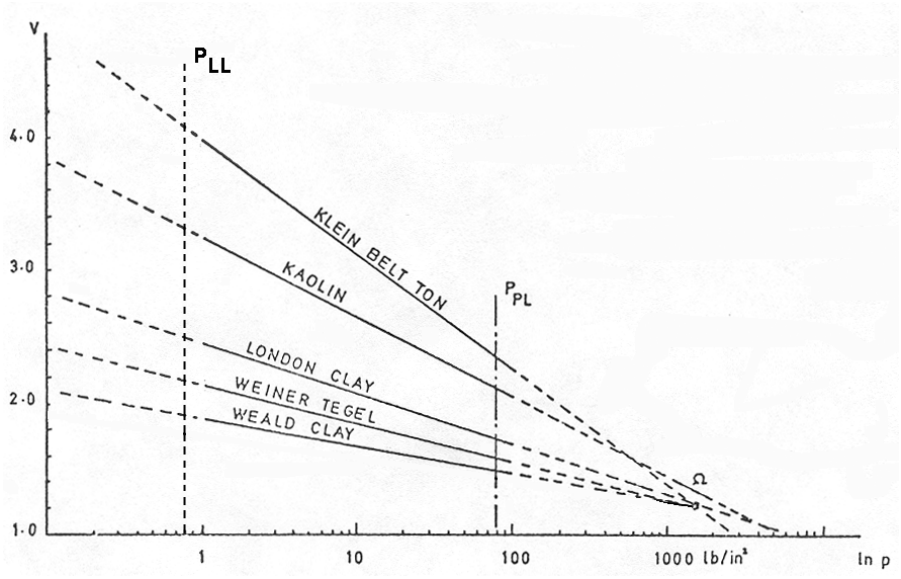

Figure 2-8: Family of critical state lines for different soils (Schofield and Wroth 1968)

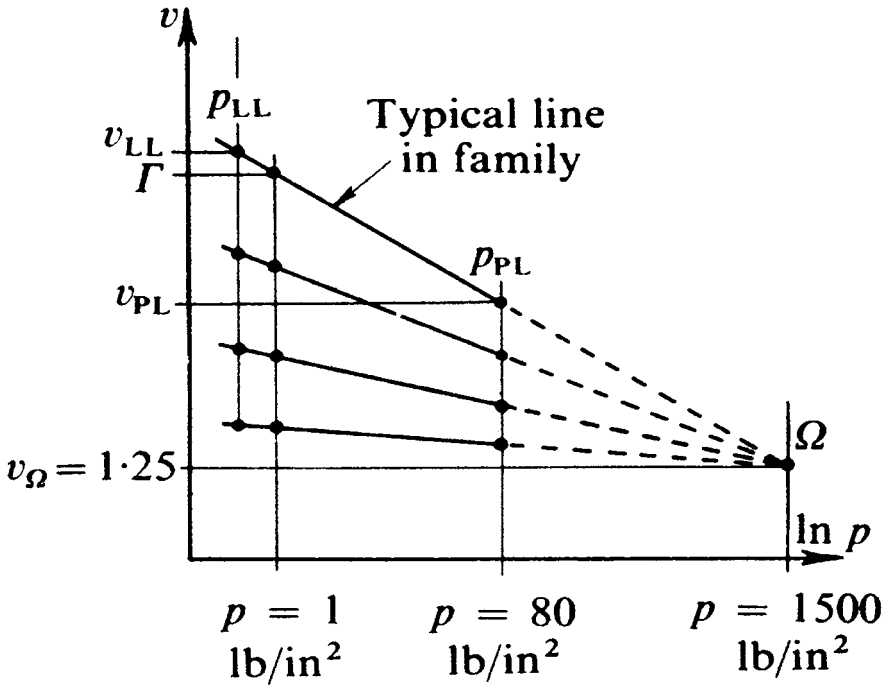

Figure 2-9: Idealized critical state lines

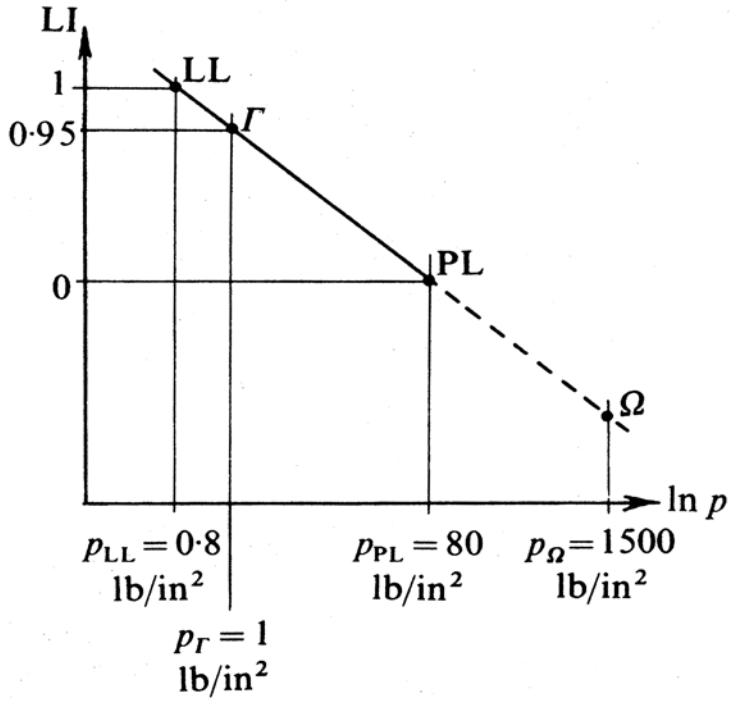

Figure 2-10: Normalized critical state line

Similarly, compression lines in v-lnp' space can be converted into LI- lnp' space using the method explained above. There are some advantages to using LI as an ordinate over v. The region of yield and rupture are small (fraction of LI) and covers a large range of pressure. Also, as it is a normalized diagram, it can readily be used for any soils with minor changes.

2.8 Limits states based on liquidity index and confining stress

In his Rankine lecture, Schofield (1980) mapped the remolded soil behavior on a liquidity against pressure diagram as shown in Figure 2-11 utilizing the hundred fold increase in pressure from liquid limit critical state to plastic limit critical state which is two log cycles. Note that the critical pressure is about 5 kPa (≃ 0.8 psi) at the liquid limit and 500 kPa (≃ 80 psi) at the plastic limit. In this plot the rupture band will become half the width of liquidity and will intersect the line $p' = 5$ kPa at LI=0.5. This intersection is a consequence of putting the lower limit of Coulomb rupture at $p'/p'_{crit} = 0.1$ (Schofield, 1980). The cam-clay yielding band is quite narrow, and corresponds to only about 0.16 liquidity ranges. Therefore, in the LI- lnp′ space, clear boundaries exist that separate regions of fracture, rupture and ductile behavior. This is an independent and convenient approach to separate the states of fracture/rupture/ ductile yield behavior of the soil using its physical properties.

Considering a body of soil initially at LI = 0.5 and subjected to an elastic compression the map suggests at shallow depths where $p' < 5$kPa there may be cracks, but for depths where 5 kPa $< p' <$ 50 kPa the soil will remain water-tight while

deforming. In contrast a body of soil initially at LI= 0 will undergo fracture at depths for which p < 50 kPa or about 3 m of the overburden depth. In other words, the overburden depth should be larger than 3 m to ensure that deformation causes rupture planes (water tight) rather than open cracks. If LI= -0.25, the depth could be about 100 kPa or 6 m of depth.

In order to identify the band of behavior in which various states of soil lie in the LI-p' space, Schofield (1980) defined their equivalent liquidities by projecting these states in the direction parallel to the critical state line towards the ordinate through $p' = 5$ kN/m^2. The equivalent liquidity LI_5 can be shown to be $LI_5 = LI+1/2 \log (p'/5)$ (Schofield 1980). Therefore, the equivalent liquidity equals liquidity as found in the ground plus a correction for stress. A value of LI_5 of less than 0.5 generally would indicate the fracture zone. Values of 0.5 to 1.0 represent the rupture zone. Values larger than 1.0 represent Cam-clay ductile zone.

Figure 2-12 shows the section of the map at constant p'. Stress ratios will increase as equivalent liquidity falls. In the high equivalent liquidity range, stress ratio increases linearly as liquidity of original cam-clay falls. The Hvorslev surface gives the rupture limits which allow higher stress ratios as one approaches lower value of p'/ p_{crit}', but at the no-tension limits, q/p'=3 in compression and –1.5 in extension. There is a general increase of limiting stress ratio as equivalent liquidity falls, but this is not a continuous change because there is a change of limiting behavior from continuous yield, to discrete rupture, to fracture of stiff fissured soil at equivalent liquidity below 0.5.

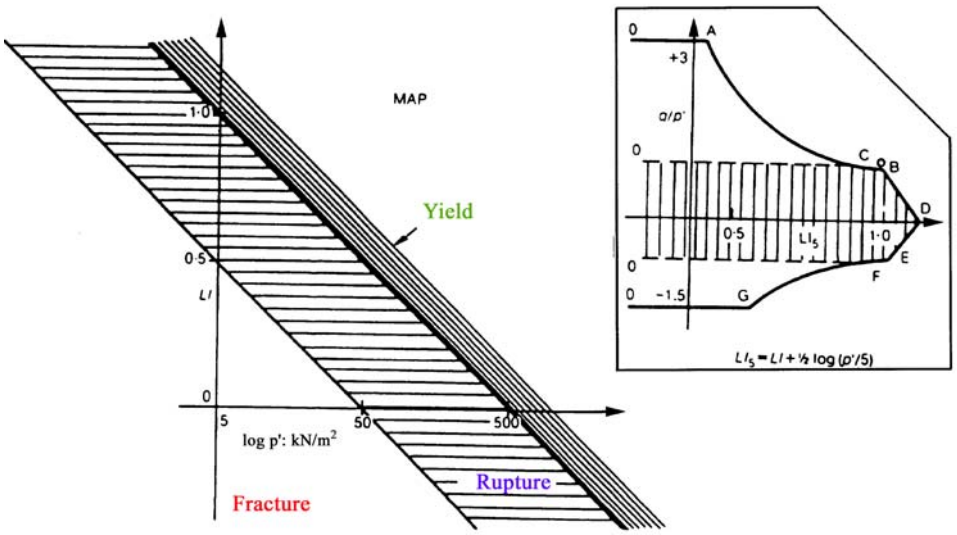

Figure 2-11: Remolded soil behavior in LI-lnp space

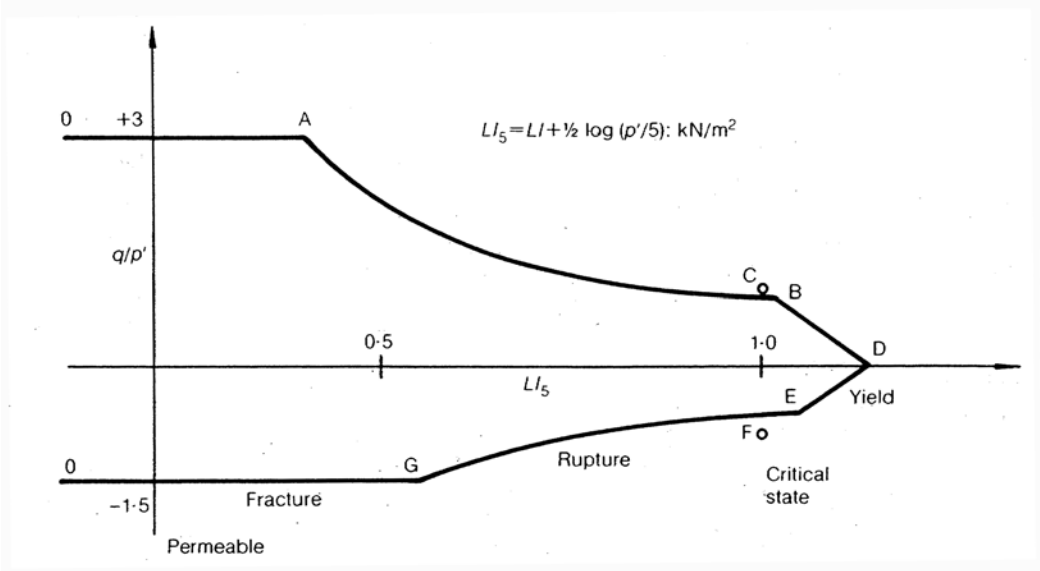

Figure 2-12: Liquidity and behavior

Figure 2-12 is a map of soil behavior with the section at constant p'. The Coulomb rupture band is about 0.5 liquidity ranges. All soil behavior depends in a major way on the density and the effective pressure. The boundaries between these bands of different behavior are only slightly different on compression and extension. In general, the combination of density and pressure that determines whether soil will fracture, rupture, or yield can be expressed by the equivalent liquidity. In a broad sense correct behavior of models will occur if all points in a model are at correct equivalent liquidity.

2.9 Summary

It has been shown that the behavior of soils depends on its states in the q/p'-p' stress space. In stress space, if the q/p' ratio is equal to or greater than 3, it indicates that the soil is prone to develop fissures or cracks. A ratio of $q/p' < 3$ indicates the soil state to be in the stable Hvorslev regime or Cam-clay yielding regime. Similarly, in the LI_5- lnp' diagram if the equivalent liquidity, LI_5 is less than 0.5, then soil is prone to fracture. If the value of LI_5 is greater than 0.5 the soil state falls in either the zone of rupture or yielding. These concepts are used in the research to explore the existence of cracks and their location in the dam.

CHAPTER THREE

TETON DAM FAILURE

3.1 History

Teton Dam was constructed by the US Bureau of Reclamation across the Teton River in southeastern Idaho approximately 10 miles (64 km) northeast of Idaho Falls (Figure 3-1). The Teton dam and reservoir were the principal features of the Teton basin project, a multipurpose project, which when completed was to serve the objectives of flood control, power generation, recreation, and supplemental irrigation water supply for large amount of farm land. It was an earth fill dam that had 405 ft (122 m) high creating 17 miles (27.4 km) long reservoir with a 436 Mega yard^3 (333 Mm^3) capacity. The construction work commenced in June 1972 and the dam was completed and first filling started in November 1975.

The dam failed during its first filling on June 5, 1976. It was the highest embankment dam that had ever failed catastrophically in the entire history of earth dam construction. At its peak release, the flow was estimated to be 37,015 yard^3/sec (28,300 m^3/sec). A wall of water rushed down the valley that was reported to be 75 ft. (22.9 m) high. Its failure resulted in 14 fatalities and an economic loss of US$400M at that time. Buildings and large areas of cropland were destroyed along with livestock down stream.

After the failure, two independent groups, the Independent Panel (IP) and the Interior Review Group (IRG) investigated the failure officially. The IP was composed of nine engineers of international repute (A.Casagrande, R.B.Peck, H.B.Seed, W.L. Chadwick, H.A.Coombs, M.W.Dowd, E.M. Fucik, R.K.Higginson, T.M.Leps, R.B. Jansen) who completed their investigation and published a report of remarkable quality in

the short time of 6 months (IP, 1976). The IRG was composed of representatives from five Federal agencies concerned with dam construction; they published two reports (IRG, 1977 and IRG, 1980). The 1980 report followed an extensive excavation along the left abutment of the dam.

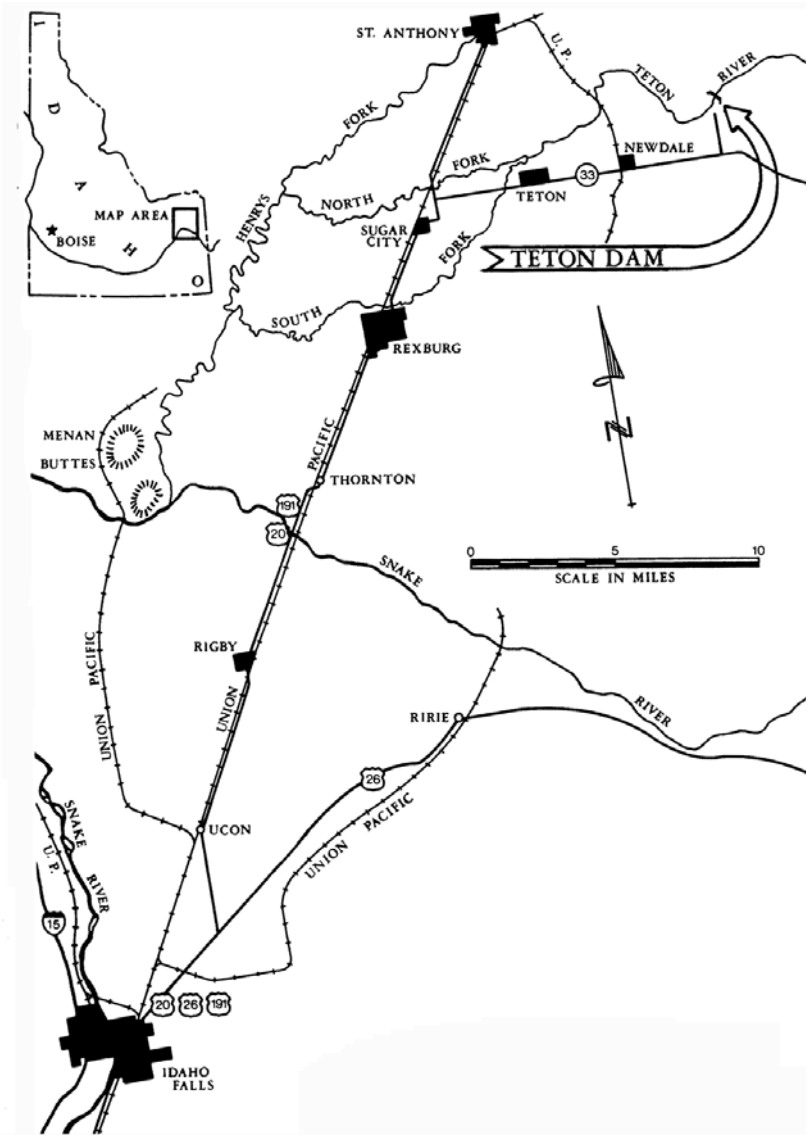

Figure 3-1: Location map of Teton Dam (IP, 1976)

3.2 Site conditions and Foundation treatment

Teton dam was located in a steep-walled canyon cut by the Teton River into a volcanic plateau known as the Rexburg Bench. A cross-section of the canyon approximately along the longitudinal axis is shown in Figure 3-2. The walls of the canyon consist of later Tertiary rhyolite welded-tuff, which is strongly jointed, with joint widths varying at different elevations typically between ¼ and 3 inches but with occasional joints up to 12 inches wide. Alluvium had been deposited in the river channel to a depth of about 100 ft. (30 m) and the high lands near the ends of the dam are covered with an aeolian silt deposit up to about 30ft. (9 m) thick. The primary features of the site are the extensive joint system in the rhyolite-tuff, which makes it extremely permeable, and the abundance of the wind-blown silt deposit, which led the designers to use substantial quantities of this material in the dam cross-section.

Extensive site exploration was performed prior to construction. Percolation tests and pumping tests revealed that the joints were capable of transmitting volumes of water over 100 gallons/min. These investigations indicated the presence of an extensive interconnecting system of joints, which made the rock extremely permeable and indicated the need to seal the joints in order to reduce the leakage to acceptable quantities. In order to investigate the possibility of sealing the upper foundation rock by grouting, an extensive pilot-grouting program was conducted on the left abutment. After the pilot grouting, the area was core-drilled and water pressure tested. Since amount of grout needed was a tremendous amount, it was concluded that it would be more economical to remove the top 70 ft. rock in the abutments above El.5100 and incorporate a deep key trench to prevent seepage.

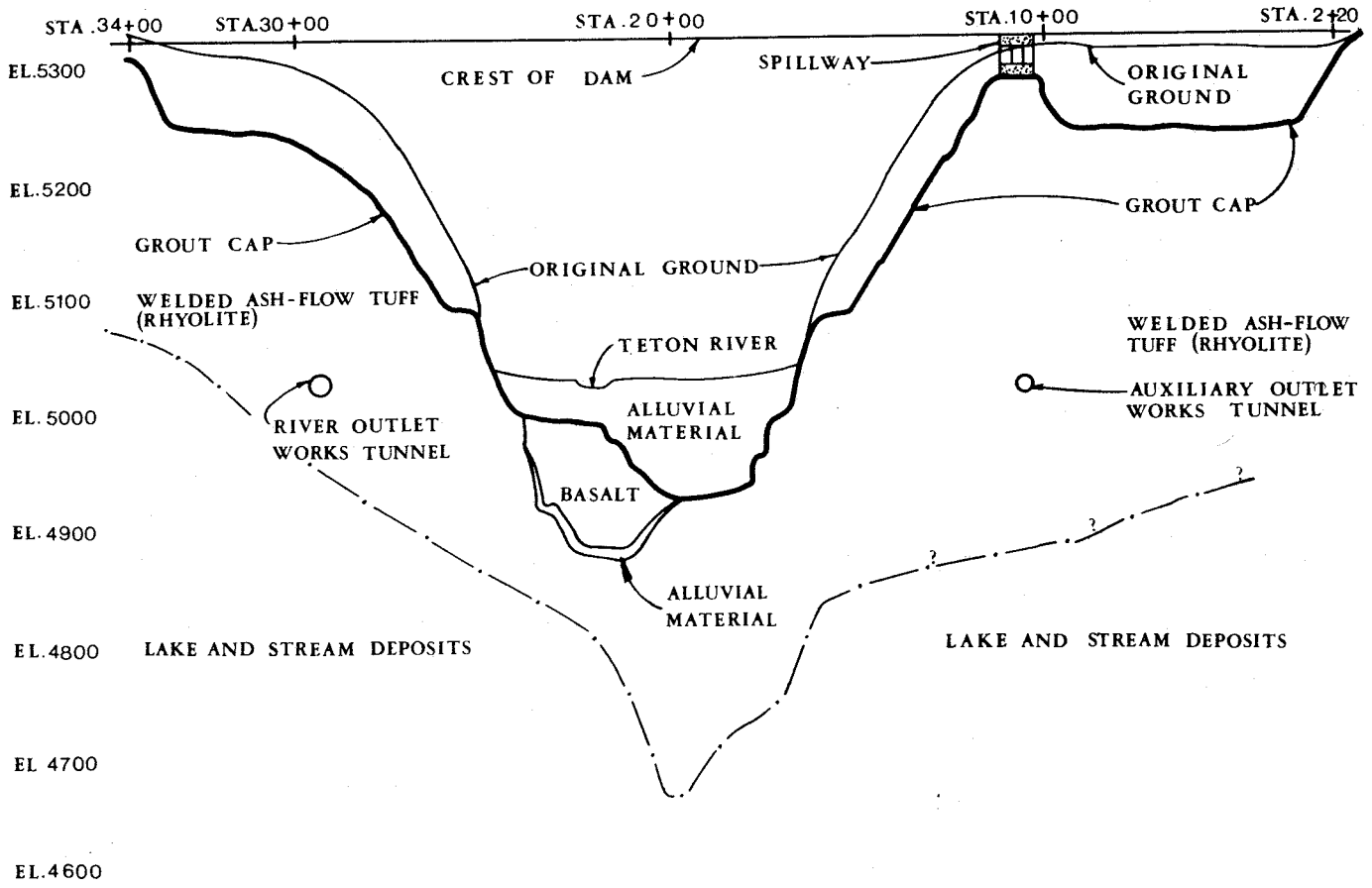

Figure 3-2: Details of deposits on a cross section of the dam (IP, 1976) (Exaggerated figure)

3.3 Embankment design

Based on the site conditions, the final design cross-section of the Teton dam at the river valley and the right abutment selected were as shown in Figures 3-3 and 3-4, respectively. The dam was conservatively designed to have a wide impervious core with a head to width ratio of about 1.5 in the upstream and 1 in the down stream (Figure 3-3). The impervious core (Zone-1) of the dam consisted of clayey silts of aeolian origin with low plasticity (PI ~ 4) and USCS classification of CL- ML and it was supported by upstream and downstream shells (Zone-2) consisting mainly of sand, gravel and cobbles. As per the design and specifications Zone-1 material was placed at an average water content of 1.0% dry of optimum and compacted to a maximum dry density of 98-102 % of the Standard Proctor test. Similarly the support zone (Zone-2) (chimney filter/drain) was compacted to a high relative density of the order of 65-70 % (IRG, 1980).

In the main section of the dam, the impervious core was extended through the foundation alluvium by means of a 100ft. deep cut-off trench backfilled with silt. On the abutments above El.5100, a similar section was adopted but key trenches with a base width of 30ft. and sides slopes ½ on 1 were excavated through the upper 70ft. of permeable rock and backfilled with clayey silt material used in the core of the dam.

Downstream of the core was a drainage zone of selected sand and gravels (Zone-2). However, no transition zone was provided between the core and the sand and gravel, nor between the impervious core and the riverbed alluvium or between key trench fill and the bed rock walls on the downstream side of the key trench. The core material in the key trench was placed directly against the rock using special compaction of a 2 ft. wide zone

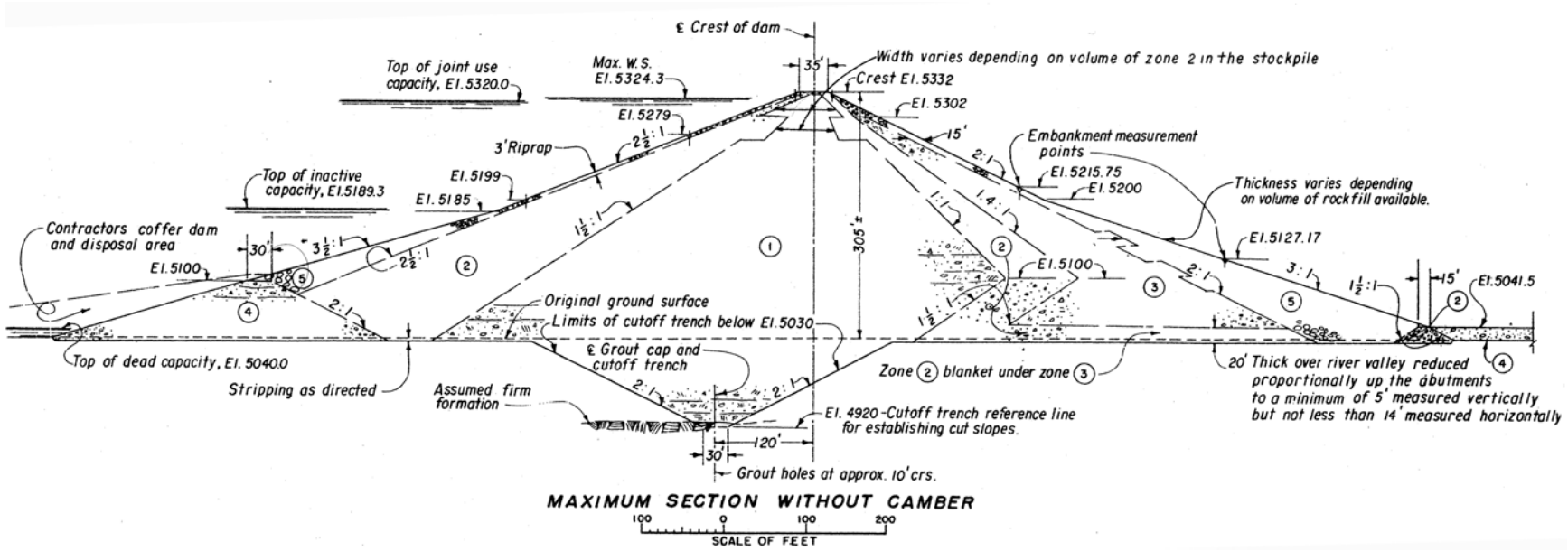

Figure 3-3: Design cross section of the dam at river valley section (IP, 1976)

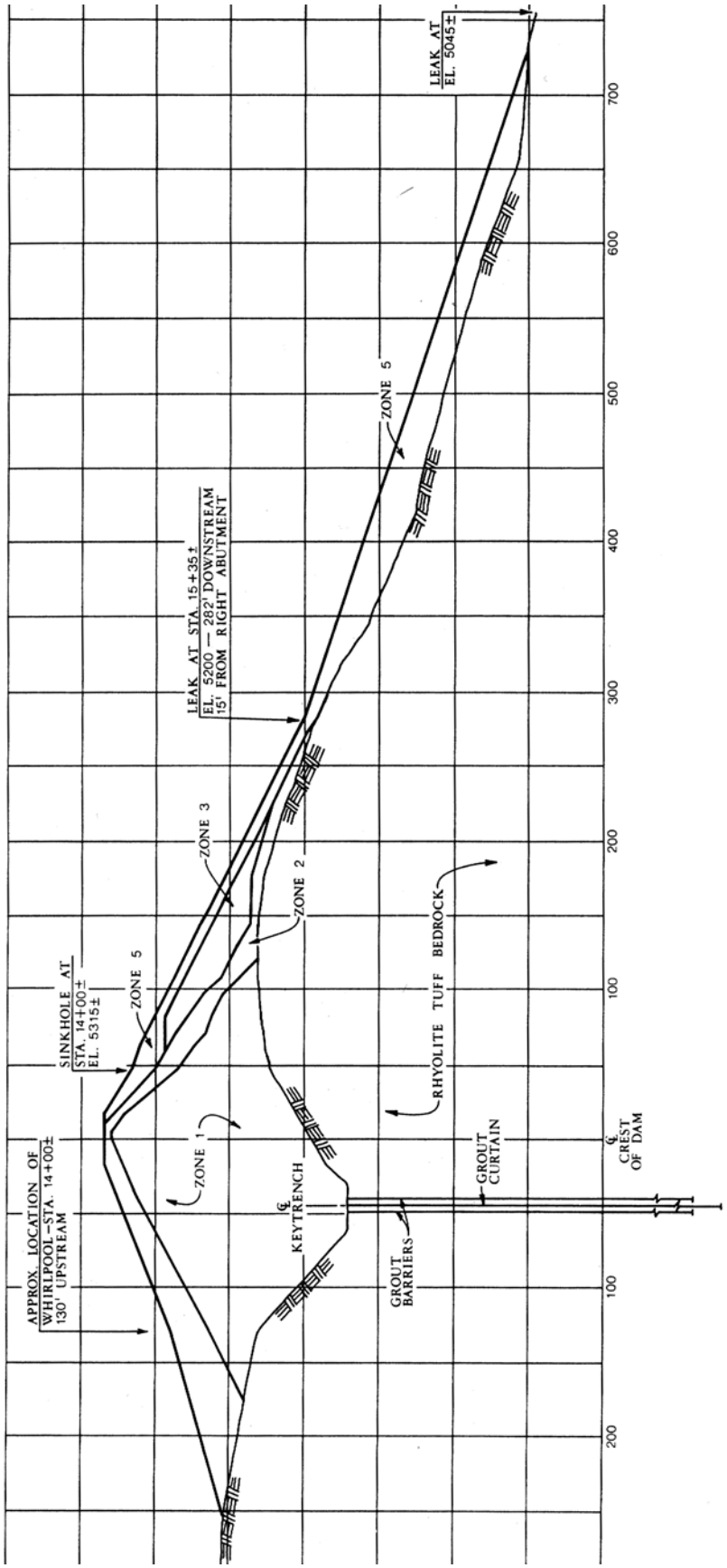

Figure 3-4: Cross section of the dam at the right abutment (IP, 1976)

of core material placed at water content above optimum. Compaction of this zone was by hand-operated compactors or rubber-tired equipment.

In addition, the design required the joints encountered in the bottom of the key trench be treated by cleaning and low-pressure grouting. A grout curtain was also installed along the full length of the dam. Lines of barrier holes intended to prevent excessive flow of grout from the main grout curtain were installed on 20 ft. centers 10 ft. upstream and downstream of the main grout curtain. To prevent seepage, the key trenches and grout curtain were continued well beyond the ends of the embankment, the curtain extending 100 ft. into the right abutment and 500 ft. into the left abutment (H.B. Seed, 1987).

3.4 Reservoir filling and the failure

Reservoir filling began in November 1975 and the water level began to rise rapidly during the spring of 1976. It was intended that the filling rate would be restricted to one foot per day, but a heavier than expected spring run-off from the watershed together with the a delay in completing outlet works led to a much higher rate of filling which during May 1976 reached about four feet per day. By June 5, the day of the failure, the water level stood at El.5302, just 3 ft. below spillway crest elevation and 30 ft. below the embankment crest.

On June 3, two days before eventual failure, some small springs flowing in total of about 100 gpm were observed at the riverbed level about 1500 ft. downstream from the embankment. On June 4, some additional springs with a flow of about 20 gpm had developed about 400 ft. from the down-stream toe. An inspection of the upstream and

downstream slopes of the embankment at about 9h00 pm that night showed no unusual condition however.

On June 5 at about 7h00 am, when the first workers reached the site, water was observed to be flowing from the downstream face of the embankment about 130 ft. below the crest (at about El.5200, Figure 3-5). The flow of about 2 ft.^{3} per second was coming from a point near the junction of the embankment and the abutment at about Station 14+00 on the right abutment. At about the same time a flow of about 25 ft.^{3} per second was observed emerging from the talus near the toe of the embankment.

The water in this latter flow was clearly dirty. In the next three hours the rate of flow from the higher elevation gradually increased to about 15 ft.^{3} per second and at about 10h30 am, one eyewitness reports a loud burst and coincident of the seepage to a point about 15 ft. in from the abutment. From this time onwards the seepage increased rapidly accompanied by progressive upward erosion; at 11h20 am the eroded hole in the dam was so large that bulldozers sent to fill the hole sank into the flow, and at about 11h55 am the dam crest was breached as a complete failure occurred.

3.5 Investigations by the independent panel (IP 1976)

IP concluded in its report (1976) that two triggering mechanisms were most likely to have led to the failure. A number of hypotheses were developed for the failure mechanisms from which the two probable mechanisms were chosen after a thorough site investigation.

The first hypothesis was that seepage under the grout cap in unsealed joints in the rock could have led to erosion along the base of the trench and thereby to a piping failure

through the key trench fill. The tests done at the site revealed the presence of a number of joints between Stations 13+00 and 13+90 beneath the grout cap through which water could pass freely. If this were the case, however, persistent water leaks would have occurred a few months before the actual failure. No such leaks were observed prior to the failure.

Figure 3-5: Initiation of the failure

The second was that a piping failure caused by seepage through cracks in the key trench fill caused by hydraulic fracturing or differential settlement. For this purpose hydro-fracturing tests were performed in drill holes made into the unfailed portion of the embankment to determine the water pressures required to cause fracturing. At the same time finite element analyses were made to determine the stress distribution in the embankment. Based on these analyses and tests, the probable stress distribution could be evaluated in the section where failure had occurred and thereby assess the possibility of

hydraulic fracturing in the core of the dam due to water pressure on the upstream. It was considered that fracturing might occur if the water pressure exceeded the sum of the transverse normal stress and the tensile strength of the soil. Theoretical stresses were compared in several sections of the embankment and it was concluded that hydraulic fracture could possibly have occurred in the range of Stations 13+70 to 15+00.

However, their experimentation to cause hydraulic fracture in the field did not succeed. The state based soil mechanics along with the results obtained from this study explains the difficulty in achieving hydraulic fracture by reservoir seepage. (See Chapter 6). Muhunthan and Schofield (2000) showed that a hydraulic fracture is not tenable from given the rigid geometry of the Teton trench.

The IP stated in their report that although they described two main triggering mechanisms for the initiation of failure, they did not provide a final answer to the specific cause of failure of Teton dam. They argued that clearly many aspects of the site and the embankment design contributed to the failure, but because the failed section was carried away by the flood waters, it would probably never be possible to resolve what would have been the primary cause of leakage in the vicinity of Station 14+00 from the described failure mechanisms.

3.6 Investigations of the interior review group (IRG 1977)

The IRG conducted its own studies but shared information with the Independent Panel issued report in 1976. The primary conclusions of this report focused on the mechanism of failure and stated "Teton Dam was constructed as specified and failed as a result of inadequate protection of Zone 1 impervious core material from internal erosion.

The most probable physical mode of failure was cracking of Zone 1 material that allowed the initiation of erosion; however the erosion could have been initiated by piping at the contact of Zone 1 and the rock surface.

However, the IRG recommended to perform additional investigations that are (1) further testing of grout curtain; (2) excavation of the left remnant of the dam to allow inspection of the embankment-foundation contact surface and to search for cracks; and (3) finite element analysis of the stress conditions on the left abutment and supporting study of the relevant parameters.

Wet seam theory

During the excavation of the left abutment of the dam a thin layer of very high water content was found and water was also found to be seeping from the exposed face of this zone. The zone was termed as a "wet seam". Borings were drilled at several sections in the remaining embankment to investigate this phenomenon. Wet seams were found in those sections and in some sections there were a multiple of them. The discovery of this extensive wet seam on the left side of the embankment immediately led to the speculation that a similar seam on the right side of the embankment may have been responsible for triggering of the failure of the dam.

Leonards and Davidson (1984) hypothesized that the wet seam materials must have been compacted well on the dry side of proctor optimum moisture content. According to them, the wet seam were initially dry seams when first compacted, and subsequently were wetted by seepage. It was further hypothesized that, as the initially dry seams were wetted, they would have tended to collapse, leading to formation of a crack or hydraulic fracture through the base of the key trench, followed by rapid erosion

and piping of the key trench fill into open joints in the down stream wall of the key trench. Upon further investigations of this aspect, they proposed the following mechanism of failure: " Subsidence or 'collapse' of a permeable dry-side compacted layer spanning the width of the key trench on the right trench fill thereby allowing flow through the open joints in the upstream wall (with access to the reservoir) to open joints in the down stream wall".

However, enormous confining stress due to the height of the dam would bring the state that was compacted dry of optimum into a more ductile state when wet by seeping water. There is no possibility for collapsing, and thereby hydraulic fracturing. (See Chapter 6 for more details).

3.7 Summary

All the mechanisms for initiation of failure suggested by both IP and IRG were concentrated at the level of embankment-rock contact. Although the suggested mechanisms seemed plausible, they had many drawbacks in describing the initiation of failure. The drawbacks are described in more details in Chapter 6. Moreover, both IP and IRG did not consider the possibility of presence of cracks in the upper potions of the embankment.

Highly compacted soils of low plasticity tend to crack in an environment of low liquidity index, low confining stresses and high shear stresses. The geometric condition of the valley section and the increased compressibility of the core material with increasing confining stress may have led to tension cracks in the upper part of the embankment. The cracks may have been inches to several feet deep.

CHAPTER FOUR

EXPERIMENTAL PROGRAM

4.1 Materials and Methods

The experimental program in this research was designed to determine both mechanical and physical properties of the core material of Teton dam. About 1000 lbs of the zone-1 material was obtained from the remnants of the failed Teton Dam. Tests for physical properties included grain size, plasticity (Atterberg) limits, and proctor compaction curves. Mechanical tests included triaxial tests on remolded soils, and consolidometer compression curves on compacted samples at w_{opt}-1, w_{opt}, and w_{opt}+1 to obtain constrained modulus at various confining stress levels.

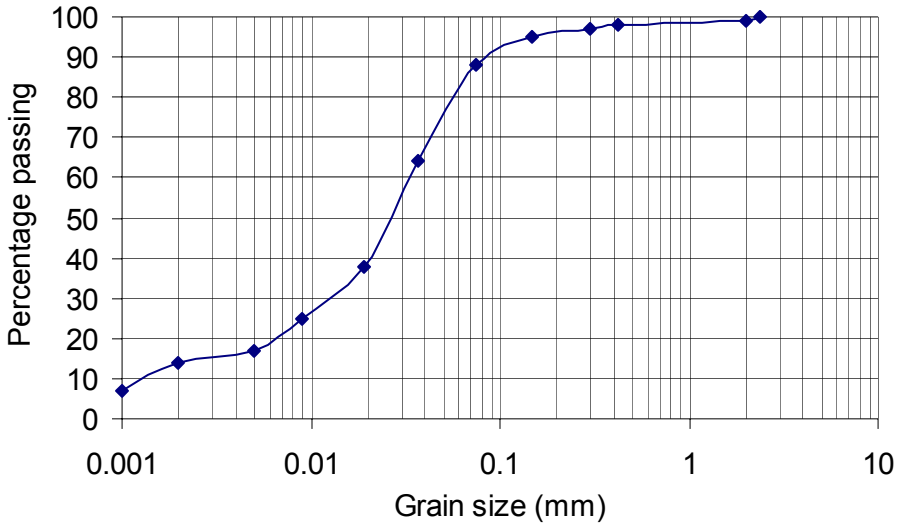

Figure 4-1: Typical grain size distribution of Teton core material (IRG, 1980)

Figure 4-1 shows the grain size distribution. The soil material that formed the impervious core of the dam (Zone 1) was derived from aeloian deposits and consisted of uniform clayey silt, 88 percent passing through #200 sieve and about 13% of clay fraction (<2 micron) and USCS classification of CL- ML.

4.2 Atterberg limits

Liquid limit (LL) and Plastic limit (PL) of the Zone-1 material were determined from Atterberg limit tests. The percussion cup (Casagrande method) method was adopted to determine the liquid limit. As the soil has very low plasticity, it was very difficult to cut a groove smoothly below the LL. Therefore, most points were obtained at water contents above the LL. The results were extrapolated to get the actual LL. The Figure 4-3 shows the liquid limit results in water content- log (number of blows, N) space. The average liquid limit is about 27 %.

Conventional rolling thread method was used here to find the plastic limit. Since this is a difficult task with low plasticity silt, a number of tests were performed and an average plasticity limit of 23 % was determined.

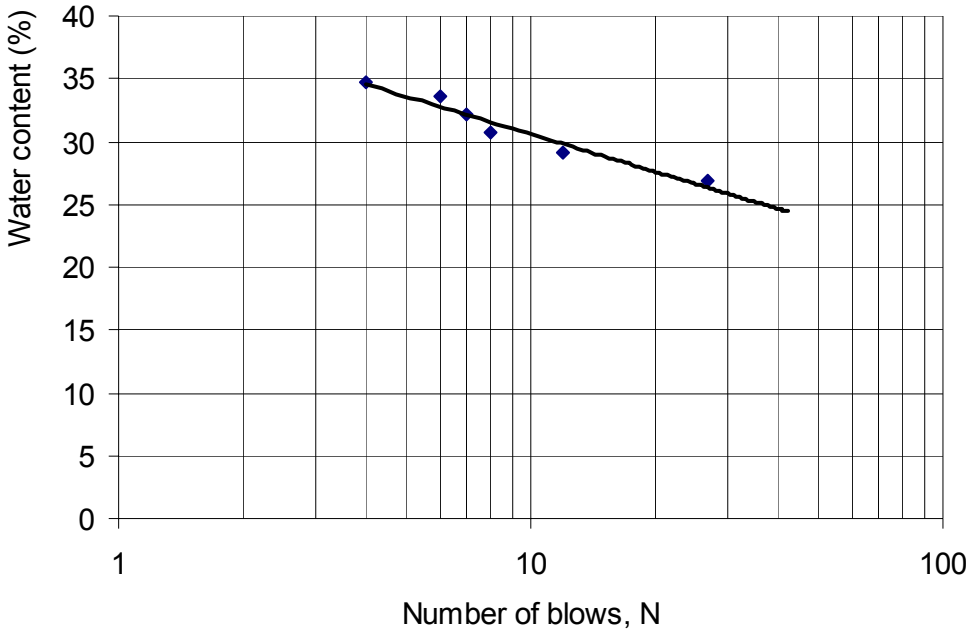

Figure 4-2: Graph of water content Vs. Number of blows of core soil

4.3 Critical State line of Teton core soil

The liquid limit and plastic limit data for the Teton core material can be plotted into the v-lnp diagram following the procedure outlined in section 2.7 as shown in Figure 2-7. It can be seen that the critical state line of Teton core soil, if extended, also passes through the point Ω. Therefore the plasticity characteristics of the core material conforms well to similar materials.

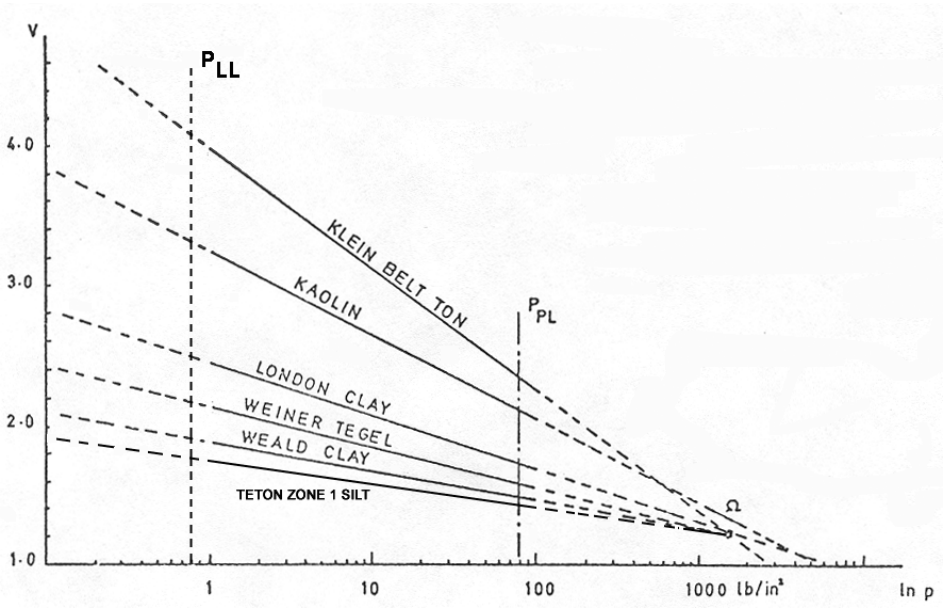

Figure 4-3: Teton soil and family of critical state lines (Schofield and Wroth 1968)

4.4 Compaction tests

Standard proctor compaction tests were carried out to determine the optimum water content and the maximum dry density of the core material. ASTM standard procedure was followed. A total of seven compaction tests were performed. One of the compaction results are shown in Table 4-3, and Figure 4-3 shows the compaction curve of Table 4-3.

The optimum moisture content varied from 17.5% to 19.6%. Similarly the maximum dry density varied from 1.61 g/cm^3 to 1.68 g/cm^3 depending on location of the samples on the embankment. Therefore, a mean design compaction curve (Fig. 4-4) was obtained. The optimum water content and the maximum dry density of the design curve are 18.5% and 1.67 g/cm^3, respectively

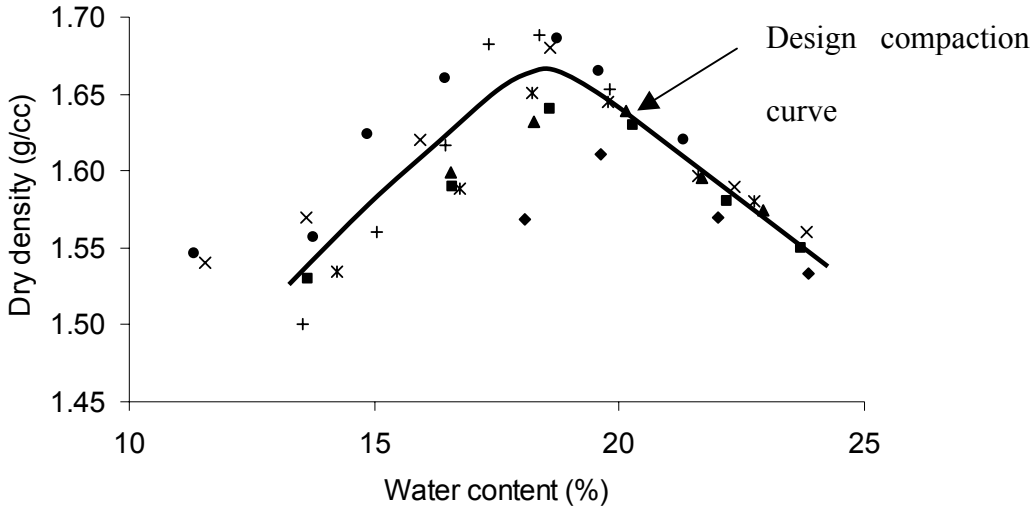

Figure 4-4: Compaction curves of Teton core material

4.5 1-D compression test

Oedometer compression tests were carried out to determine the mechanical properties of Teton soil at the water content of w_{opt}-1, w_{opt}, and w_{opt}+1. Since the mechanical properties such as the slope of compression lines need to represent the behavior of the compacted fill of the Teton dam, the specimens for the tests were obtained from the soil that had previously been compacted at certain water content in laboratory.

The soil was first oven-dried and then added water (w_{opt}-1 or w_{opt} or w_{opt}+1) and compacted using standard Proctor method. The compacted the soil was taken from the mold and trimmed to fit into the oedometer ring. It was then placed in the loading device and was loaded in intervals of 30 minutes. The maximum pressure applied was 2400 kPa. Thereafter the specimen was unloaded. Dial readings were recorded during loading and unloading. Weight of ring and wet soil before and after the test and that of ring and dry soil were also recorded.

The e-lnp' curve for the Teton material is as shown in Figure 4-4. From this graph the gradients of the compression line (λ) and the swelling line (κ) were found to be .03 and 0.005, respectively. These values compare well with the relationship proposed by Schofield and Wroth (1968) (For example $\lambda \sim 0$ .585PI). The maximum precompression pressure was obtained to about 12000 psf. (575 kPa).

4.6 Unconfined compression tests

Three unconfined compression tests were carried out for the Teton core material at the water contents of w_{opt}-1=17.5, w_{opt}=18.5, and w_{opt}+1=19.5. Specimens were compacted using the Harvard miniature compaction mold using tamping. The stress-strain curves for the three specimens are as shown in Figure 4-6. It can be seen all of the material show brittle behavior with the specimen compacted at 17.5 % showing the most brittleness. With addition of moisture (Say 19.5 %) the material tends towards more ductile type behavior.

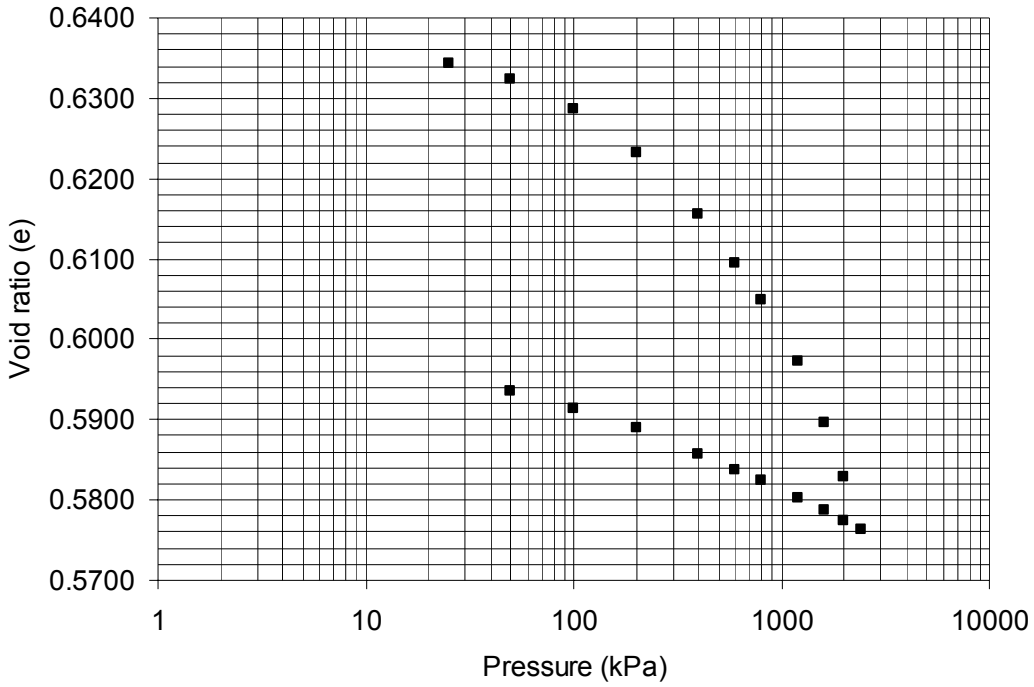

Figure 4-5: Compression curve of Teton core material

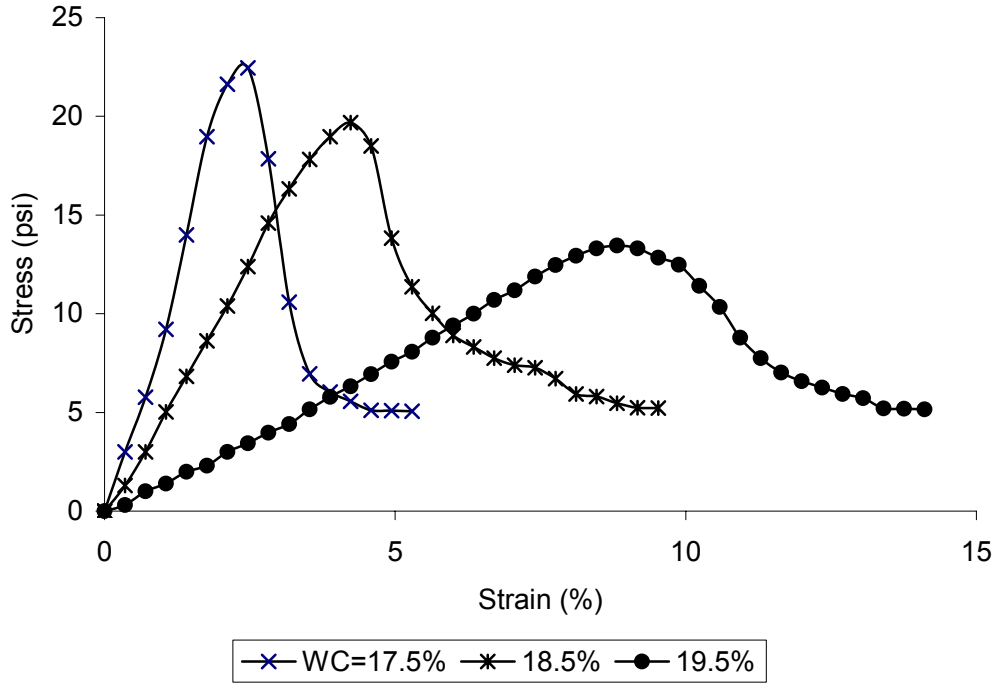

Figure 4-6: Stress-strain curves at different water contents of Teton core material

4.7 Critical State Parameter M

Direct shear tests were performed to find the critical state friction parameter M of Teton soil (Zone-1) needed for the finite element analysis. Three tests were performed at normal loads of 10, 30, 50 kPa with constant initial void ratio of 0.65. The constant initial void ratio was maintained by having same weight of soil for preparing the sample for the test.

Since the critical state of a soil is usually attained at a higher shear strain it is difficult to attain it in a direct shear apparatus due to non-uniform conditions. Therefore, this study made use of the proposal by Taylor (1948) in that the shear strength consists of critical state friction and the interlocking due to dilatancy. Accordingly, the work done in shearing is given by:

$$\tau dx = \mu\sigma dx + \sigma dy \tag{4-1}$$

where *dx* and *dy* are shear and normal displacements and τ and σ are shear and normal stress and μ is friction at critical state.

Rearranging:

$$\frac{\tau}{\sigma} = \mu + \frac{dy}{dx} \tag{4-2}$$

Hence $\mu = tan\phi$ can be obtained by correcting the measured τ/σ with the slope *dy/dx*. The typical result of the direct shear test on Teton soil is shown in Fig. 4-7, which results in critical state friction value μ of 0.56. Using this value in $M = \frac{6\sin\phi}{3-\sin\phi}$ results in a value of 1.1 for the critical state friction parameter.

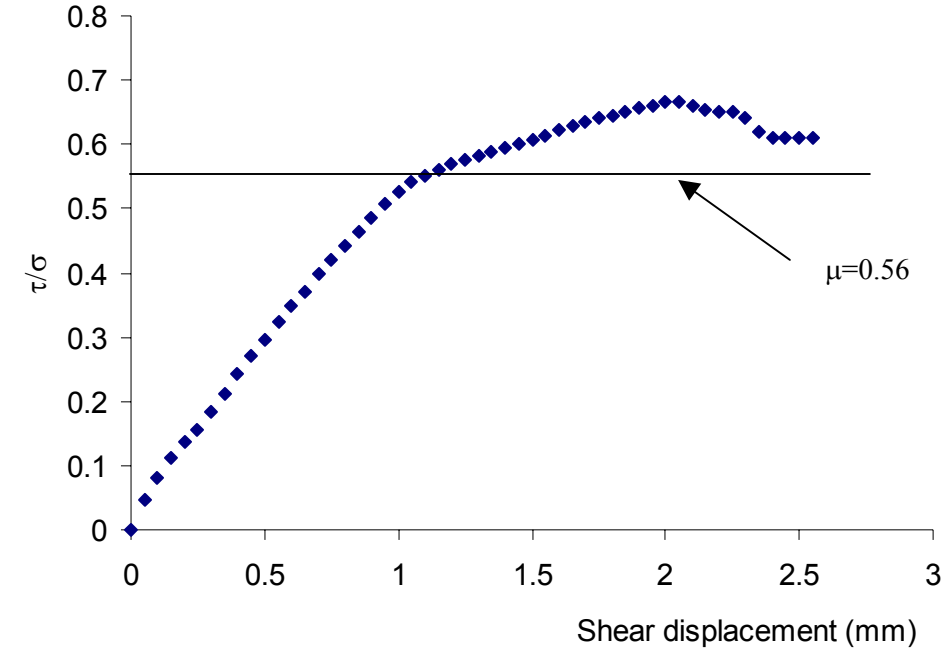

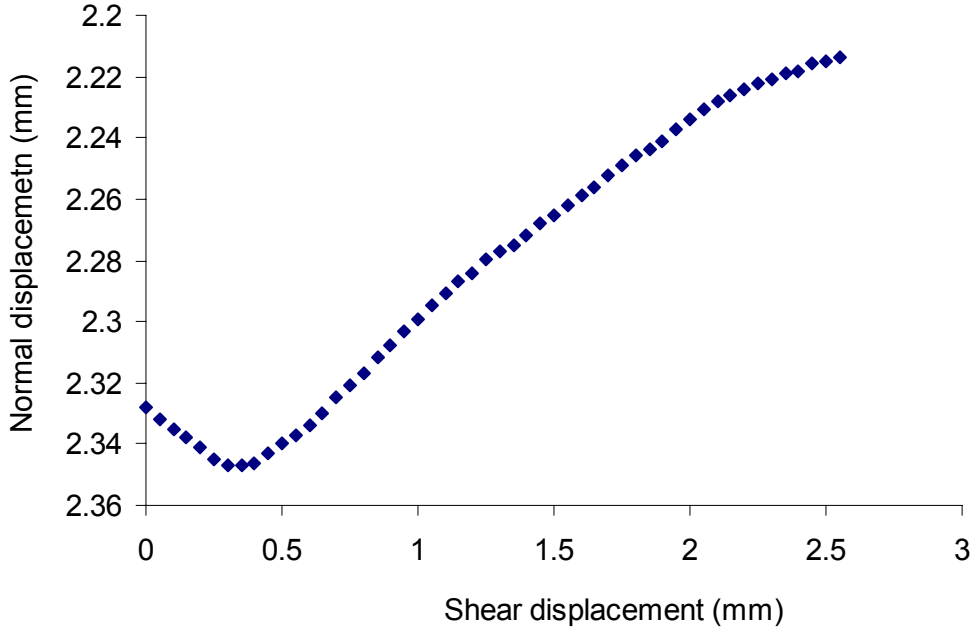

Figure 4-7: Direct shear test on Teton soil at normal pressure of 50 kPa

CHAPTER FIVE

FINITE ELEMENT ANALYSIS

5.1 Finite element method

The distribution of q and p' on the longitudinal section of the dam are needed for the analyses. Since the problem involves non-linear materials and an irregular geometry, a numerical method must be adopted. Moreover, the calculations need to be done repeatedly for parametric studies. Since the finite element method is versatile for this purpose and can include advanced soil material models, it was adopted for the stress analyses of the Teton dam.

ABAQUS, which is developed by Hibbitt, Karlsson and Sorensen, Inc., was used in the study. It is a general-purpose commercial finite element software, capable of performing linear and non-linear analyses. Moreover, it has many built-in materials for many types of analyses in its material library. The critical state plasticity model, which is an extension of the critical state models originally developed by Roscoe and his coworkers at Cambridge, is used as the non-linear plasticity model. Porous elasticity model is used to model the elastic behavior of porous materials.

In addition, the construction of an embankment can be simulated in this program using one of its special features, the * MODEL CHANGE option. Stresses can be exported to another software to draw the contours of q/p' stress ratio to determine the state of soil in the stress space.

5.2 Finite element model

The longitudinal section of the dam is shown is Figure 5-1. It can be seen that the profile of bottom of the dam has steep slopes, berms, etc. Therefore a longitudinal section was chosen for finite element analyses (FEA) as it captures all of the variation of the bottom profile. Plane strain conditions are assumed to prevail along the section.

The FE discretization is shown in Figure 5-2. The mesh elements used are four-node bilinear plane strain continuum type elements. A total of 970 elements with 1065 nodes were used. ABAQUS automatically meshes the geometry according to the given element size.

5.3 Material model

The material models used for the analyses are the critical state plasticity model and the porous elasticity model. These material models are available in the ABAQUS materials library and they can be used with the plane strain continuum type elements.

5.3.1 Critical state (Clay) plasticity model

The inelastic constitutive theory provided in ABAQUS for modeling cohesionless materials is based on the critical state plasticity theory developed by Roscoe and his colleagues at Cambridge (Roscoe and Burland 1968). The specific model implemented is an extension of the "modified Cam-clay" theory (Roscoe and Burland 1968).

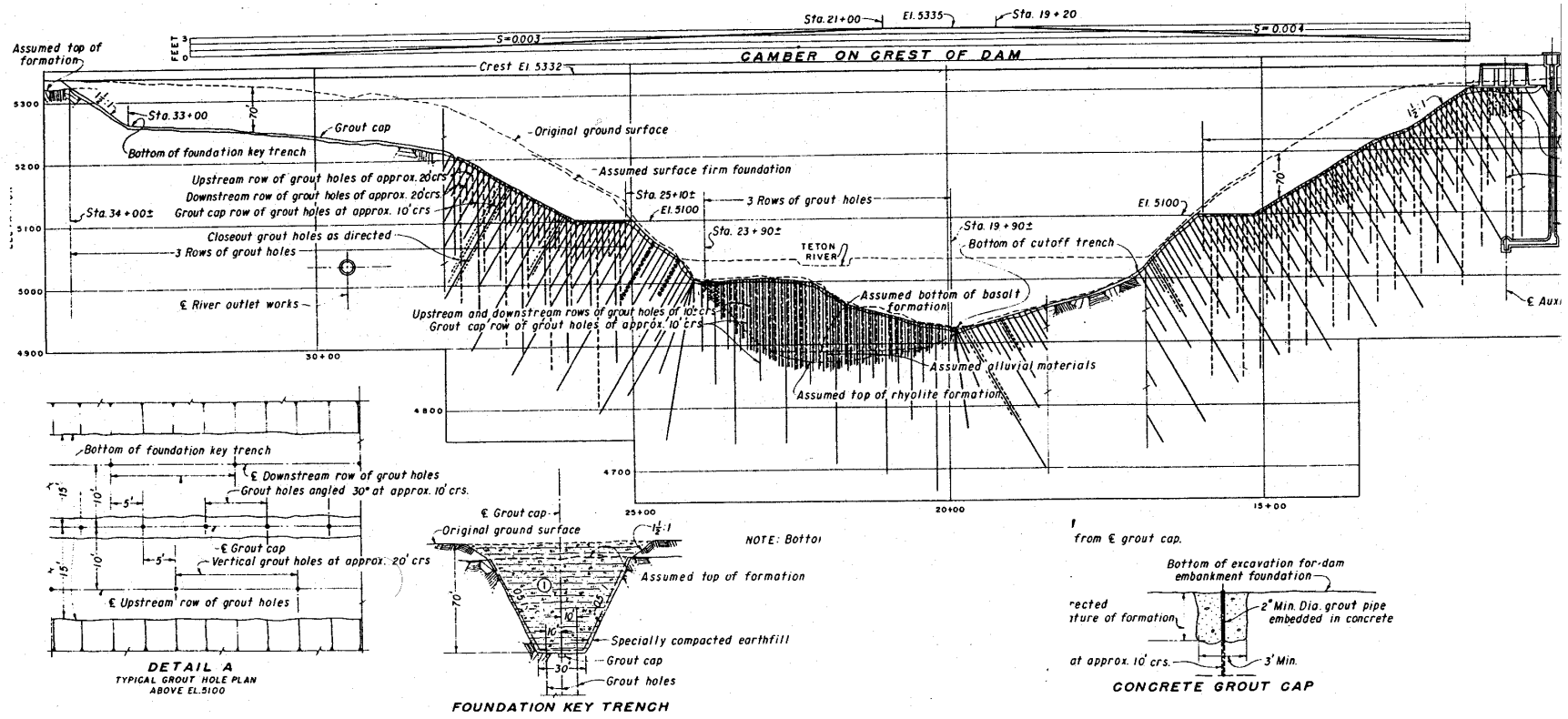

Figure 5-1: Longitudinal section of the dam along the center line of the crest

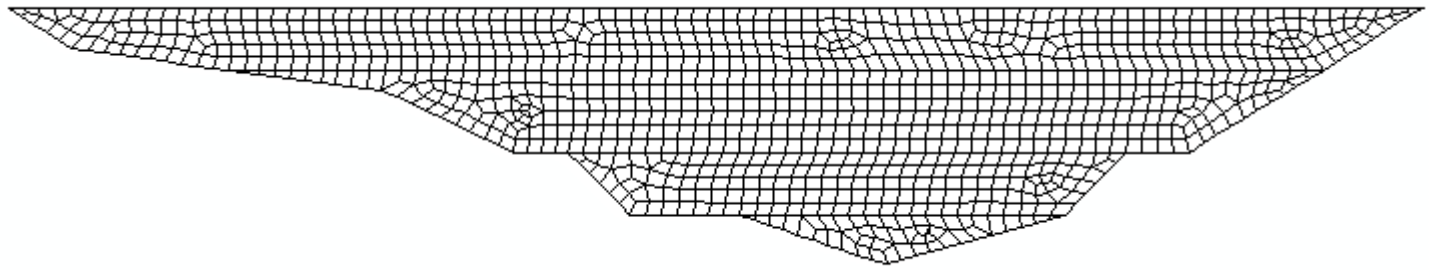

Figure 5-2: Finite element discretization of the dam

The modified Cam-clay is a classical plasticity model. It uses a strain rate decomposition in which the rate of deformation of the soil is decomposed into elastic and plastic parts. An elasticity model (either linear elastic or Porous elastic model, which exhibits an increasing bulk elastic stiffness as the material undergoes compression) is used to obtain the elastic part whereas a yield surface, a flow rule, and a hardening rule are needed to obtain the plastic part. The hardening rule allows the yield surface to grow or shrink depending on the state of the stress. The model has been implemented numerically in ABAQUS using backward Euler integration of the flow rule and hardening rule.

5.3.2 Yield surface

The yield surface in q-p space is an ellipse, whose form is given as Eq. 5-1,

$$\frac{1}{\beta^2}\left(\frac{p}{a}-1\right)^2+\left(\frac{t}{\mathrm{M}a}\right)^2-1=0 \qquad 5\text{-}1$$

where p is the mean effective stress; M is the slope of the critical state line, t is the deviatoric stress measure, a is the center of the yield surface in p-t plane and β is a constant used to define the different ellipse on the wet side of the critical state line. The deviatoric stress measure, t, is defined as:

$$t=\tfrac{1}{2}q\left[1+K-\left(1-\frac{1}{K}\right)\left(\frac{r}{q}\right)^3\right] \qquad 5\text{-}2$$

where r is the third invariant of the stress tensor and K is the ratio of the flow stress in triaxial tension to the flow stress in triaxial compression and determines the shape of the yield surface in the Π-plane (Figure 5-3). The shape can be varied by changing the K

value. K equal to unity gives the circular shape (Shape B in the Figure 5-3) and K=0.8 gives the shape A. Note that ABAQUS requires that $0.778 \leq K \leq 1.0$ to ensure that the yield surface remains convex.

The modified Cam-clay yield surface has the same shape in the Π-plane as the surface of the original critical state model (Figure 5-3), but in the *p*-*t* plane it is assumed to be made up of two elliptic arcs: one arc passes through the origin with its tangent at right angles to the pressure stress axis and intersects the critical state line where its tangent is parallel to the pressure stress axis, while the other arc is a smooth continuation of the first arc through the critical state line and intersects the pressure stress axis at some nonzero value of pressure stress, again with its tangent at right angles to that axis (Figure 5-4). Plastic flow is assumed to occur normal to this surface.

The hardening/softening assumption controls the size of the yield surface in effective stress space. The hardening/softening is assumed to depend only on the volumetric plastic strain component and is such that, when the volumetric plastic strain is compressive (that is, when the soil skeleton is compacted), the yield surface grows in size, while inelastic increase in the volume of the soil skeleton causes the yield surface to shrink. The choice of different elliptical arcs for the yield surface in the (p, t) plane, together with the associated flow assumption, causes softening of the material for yielding states where $t > M\,p$ (to the left of the critical state line in Figure 5-4, the "dry" side of critical state) and hardening of the material for yielding states where $t < M\,p$ (to the right of the critical state line in Figure 5-4, the "wet" side of critical state).

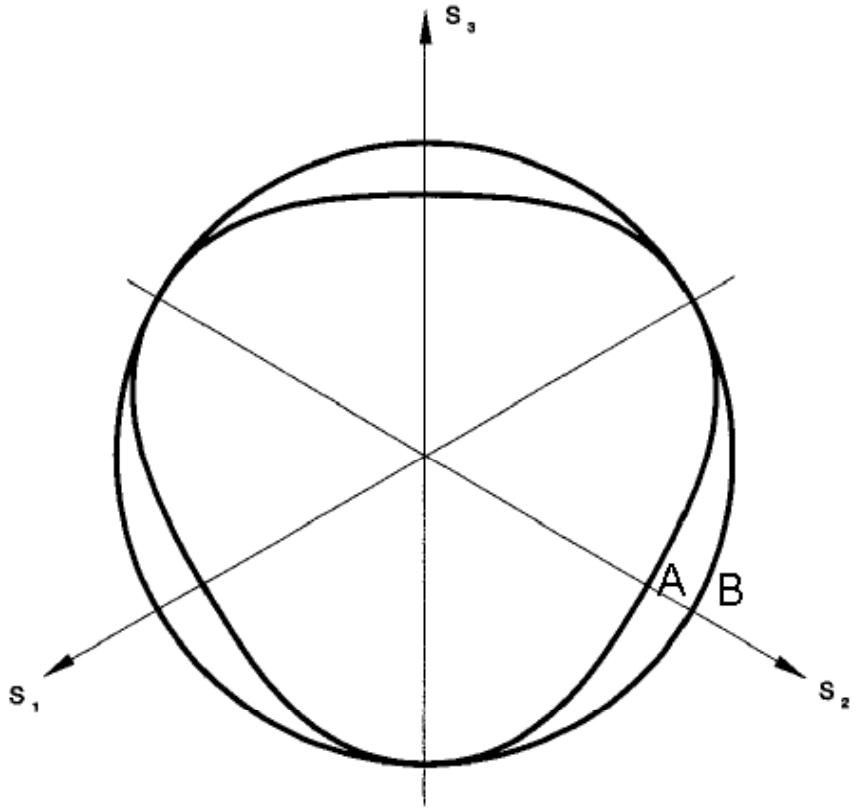

Figures 5-3: Yield surface in Π-plane (after ABAQUS)

The initial yield surface, which depends on over consolidation/over compaction, is entered before the start of the analysis through the parameter a_0, which is the initial center of the yield surface defined as:

$$a_0 = \frac{1}{2}\exp\left(\frac{e_1 - e_0 - \kappa \ln p_0}{\lambda - \kappa}\right) \tag{5-3}$$

where e_1 is the intercept of the normally consolidation line at p'= 1 kPa. Following initial yield, strain softening or strain hardening occurs until the stress state lies on the critical state surface when unrestricted deviatoric plastic flow (perfect plasticity) occurs.

The hardening law can be given in an exponential form by using the porous elasticity model or as a piecewise linear form. The piecewise hardening law is defined by using experimental yield stress-plastic volumetric strain curve.

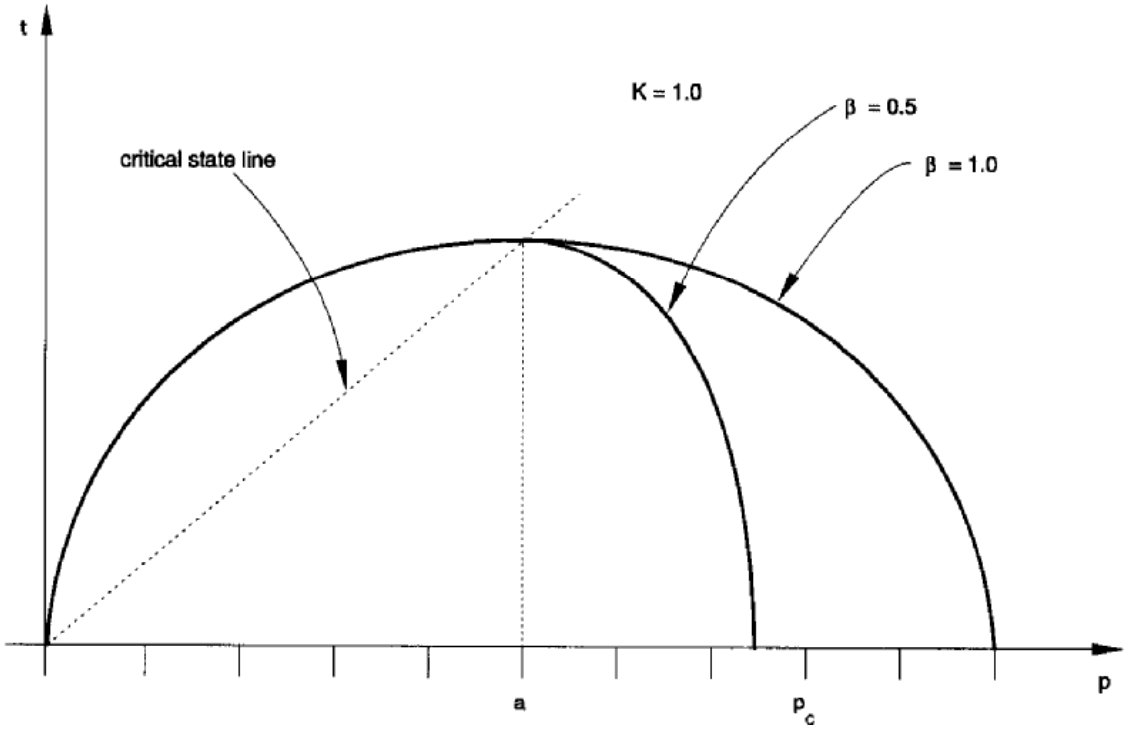

Figure 5-4: Yield surface in *p-t* plane (after ABAQUS)

5.3.3 Porous elasticity model

This model is suitable for the granular materials, which show increase in bulk modulus as they are compacted. It is valid for small elastic strains (normally less than 5%) and is a nonlinear, isotropic elasticity model in which the pressure stress varies as an exponential function of volumetric strain. The porous elasticity model is used in conjunction with plasticity models that allow plastic volume changes.

5.4 Defining the material in ABAQUS

The critical state plasticity material model in conjunction with the porous elasticity material model is defined in ABAQUS with the option *CLAY PLASTICITY. The exponential hardening law can be used only with porous elasticity material model. The material block for the ABAQUS input file should include all the options given below.

```
*INITIAL CONDITIONS, TYPE=RATIO
*INITIAL CONDITIONS, TYPE=STRESS, GEOSTATIC
*POROUS ELASTIC, SHEAR=G
*CLAY PLASTICITY, HARDENING=EXPONENTIAL
```

MATERIAL BLOCK

*INITIAL CONDITIONS, TYPE=RATIO is used to define the void ratio at all nodes of the model. *INITIAL CONDITIONS, TYPE=STRESS, GEOSTATIC is used to define the geostatic stress state inside the model. In this option the ratio of horizontal stress to vertical stress (K_0 condition) can be given to represent the anisotropy stress state at the initial stage. *POROUS ELASTIC, SHEAR=G is to define the elastic behavior of the material. Slope of the swelling curve in e-lnp space (Logarithmic bulk modulus), κ and shear modulus, G are given in the data line for this option. *CLAY PLASTICITY, HARDENING=EXPONENTIAL is to define the plastic behavior of the material. In the data line of this option the slope of compression curve in e-lnp' space (the logarithmic hardening constant) λ, the slope of the critical state line M, β and K are given. The initial size of the yield curve can also be defined in the same data line by specifying the value of

a_0. Alternatively, a_0 can be defined indirectly by specifying e_1, which is the intercept of the virgin consolidation line with the void ratio axis in the plot of void ratio, *e,* versus the logarithm of the effective pressure stress, ln *p*' in the *CLAY PLASTICITY option line.

5.5 Material parameters

Based on the tests performed on Teton soil (Chapter 4), the parameters that were needed for finite element analysis were determined. Table 5-3 gives the details of parameters that were input in the FE model. In ABAQUS, the initial yield curve is defined by its center. The precompression pressure was converted to the center of the initial yield curve by using the equation of modified cam clay yield function. The Poisson ratio, ν, was assumed to have the value of 0.3. The shear modulus was obtained from unconfined compression tests. The average density of placed soil was assumed to be 120 pcf.

Table 5-1: Material parameters for the finite element analysis

Critical State Parameter	Value
κ	0.005
λ	0.03
Γ	2.5
M	1.1
ν	0.3
G (psf)	300000
p'c (psf)	12000

5.6 Analysis procedure

Two types of analysis techniques were adopted in the finite element analysis of the Teton dam to simulate its construction. The first one uses the *MODEL CHANGE option in ABAQUS, which allows the removal of elements and addition of elements where necessary. The FE model of the dam was divided into four layers and each layer was assigned suitable material properties. Based on the e-lnp' diagram, it was found that the Cam-clay yielding was in the region below the depth of 100 ft because the maximum pre-compression load was 12000 psf and the density of the soil was 120 pcf.

In the first step, the top three layers were removed using *MODEL CHANGE, TYPE=ELEMENT, REMOVE option and the remaining layer was analyzed using *GEOSTATIC procedure. This was to allow the geostatic stress field to reach equilibrium with initial conditions, applied load, and boundary conditions. This is usually the first step of a geotechnical analysis, and can be linear or non linear.

Just prior to the removal step, ABAQUS stores the forces that the region to be removed is exerting on the remaining part of the model at the nodes on the interface boundary. These forces are ramped down to zero during the removal step; therefore, the effect of the removed region on the rest of the model is completely absent only at the end of the removal step.

In the subsequent steps the removed layers were added one by one using *MODEL CHANGE, TYPE=ELEMENT, ADD option. Two distinct types; strain-free reactivation and reactivation with strain are provided for stress/displacement elements in the program. The strain-free activation scheme was adopted here to avoid strain incompatibility by the deformation of the previous layer.

The second type of analysis technique uses a simpler method of simulating the construction of the dam. The same FE model used for the first technique was used. In the first step, the bottom layer was assigned with its self-weight and other layers were assigned with zero self-weight. In the subsequent steps, the self-weight of other layers were assigned. Results obtained from this analysis compared well with those obtained from the first technique. Therefore, the results obtained from the first technique were used for the conclusions of this study as they simulate the effects of construction of the dam well.

*AMPLITUDE option was used to apply gravity load incrementally in 50 steps. More steps would give more accurate results, but 50 steps for each layer was found to be sufficient to obtain realistic results.

The boundary conditions were assumed to be fixed in both directions of motions (Pinned boundary conditions). Soils were well compacted into the key trench and cut off trench (IP, 1976). Therefore, it is a reasonably good assumption that the boundary conditions were pinned.

5.7 Finite element results

The post processing of the finite element results gives the deformation shape of the model (Fig.5-5) and von-Mises stress variation on the longitudinal section of the dam (Fig. 5-6). The material models were verified by ABAQUS (See ABAQUS 6.3-1 manuals) and therefore those were directly used in the study. As a check, the vertical stresses can be verified. The Figure 5-7 shows the vertical stress distribution. The

maximum stress corresponding to the largest depth (412 ft) is 49440 psf and it compares well with the maximum vertical stress obtained from FE analysis.

Since the contours of the ratio of q/p' ratio on the longitudinal section cannot directly be obtained from ABAQUS, the values of q and p' were extracted from the output file and contours were plotted using another software called SURFACE. To draw contours in SURFACE, coordinates of points and q/p' ratio are needed. But, the output file of ABAQUS contains only nodal data and corresponding stress values. Therefore, a software code was written in the C language to arrange the q and p' values according to the coordinates. The resulting contours of q/p' ratio are as shown in Figure 5-8.

5.8 States in LI_5- lnp' Space

The state of soils can be identified using their equivalent liquidity indices (Sec.2.8). The majority of soil placement was on the dry of optimum (w_{opt}–1). Therefore, the liquidity of the placement soils were around –0.25. Using this information, along with the effective confining pressures obtained from finite element analysis, the equivalent liquidity indices (LI_5) of the soil on the longitudinal section of the dam were determined. Contours of constant LI_5 were plotted on the cross section as shown in Figure 5-9.

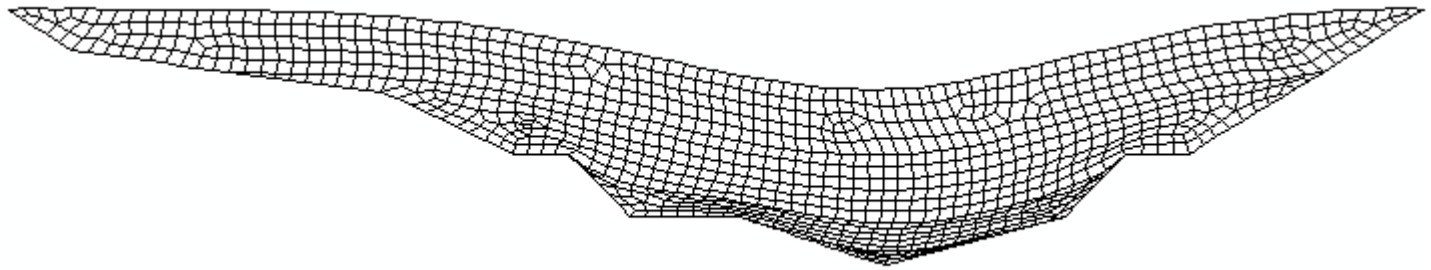

Figure 5-5: Deformed shape of Teton dam under its self-weight

(Deformations were exaggerated in the Y direction)

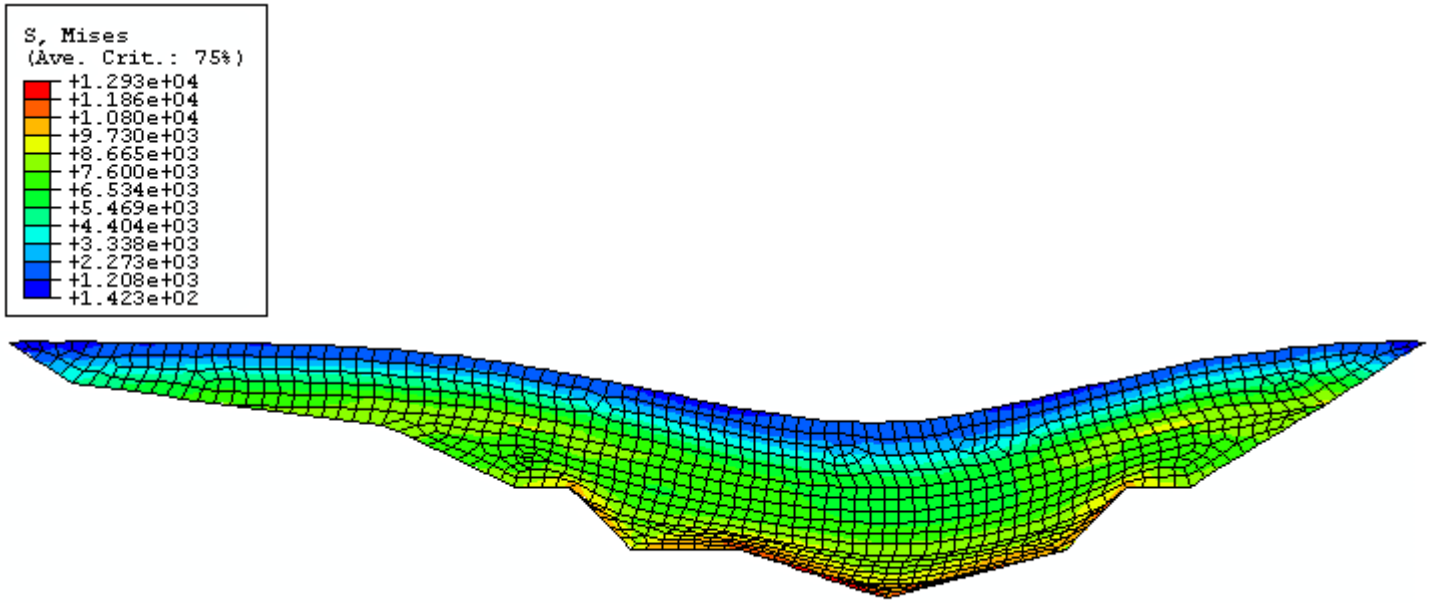

Figure 5-6: von-Misee stress distribution on the longitudinal section

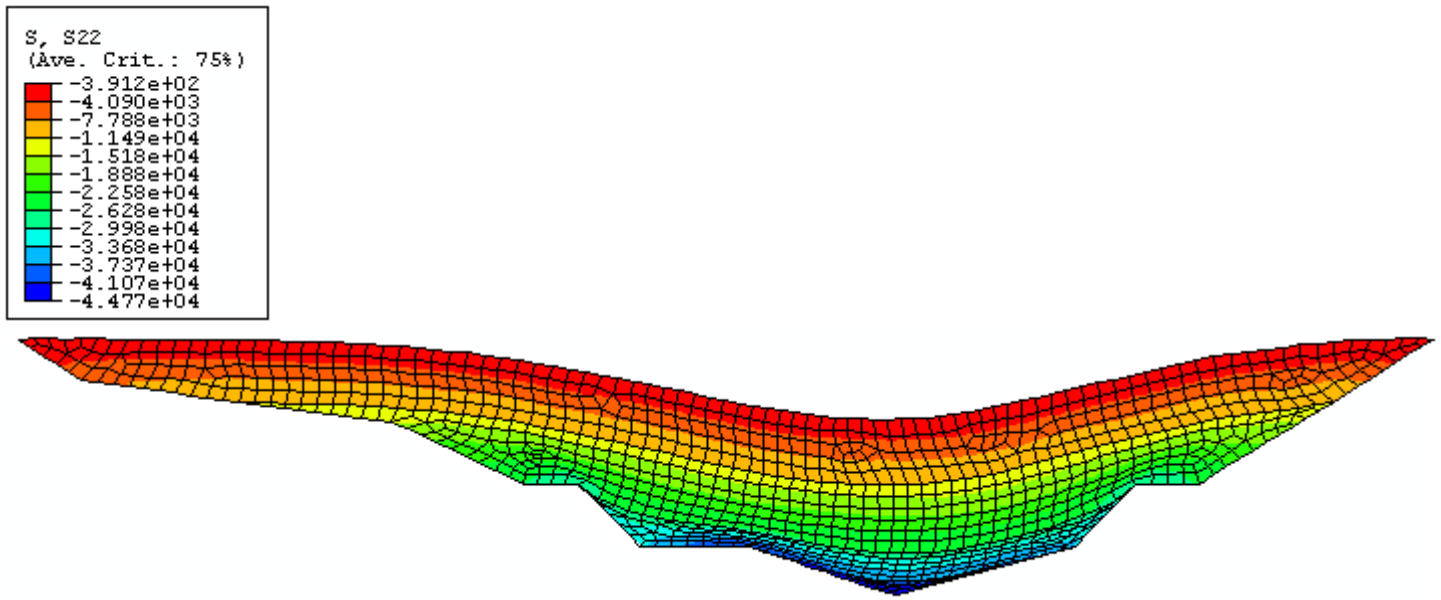

Figure 5-7: Vertical stress distribution on the longitudinal section

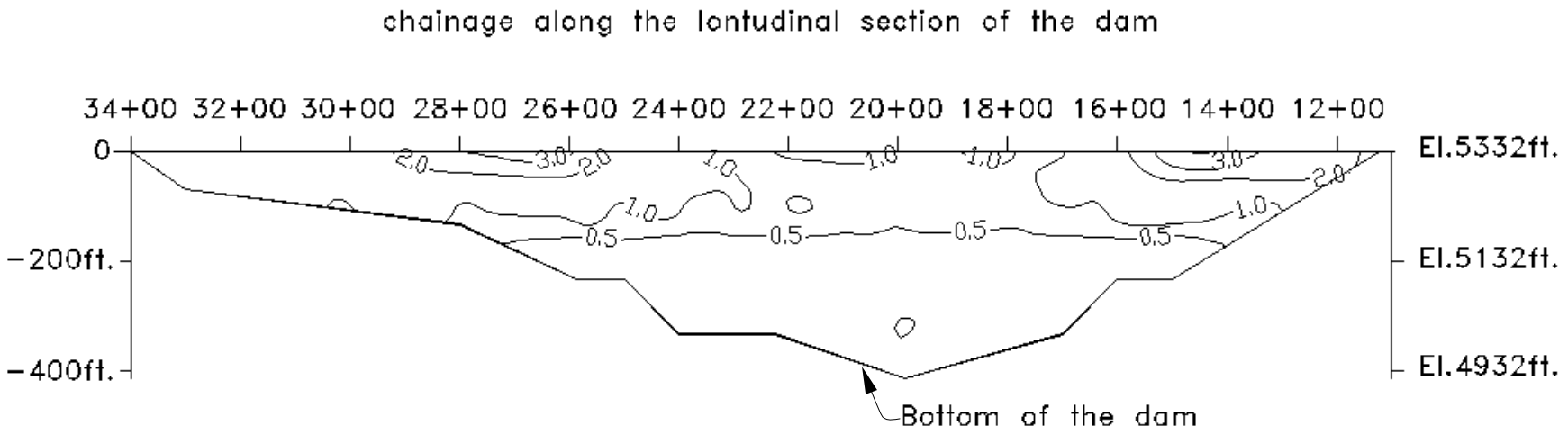

Figure 5-8: Contours of q/p' ratio on the longitudinal section of the dam, (One chainage= 100 ft.)

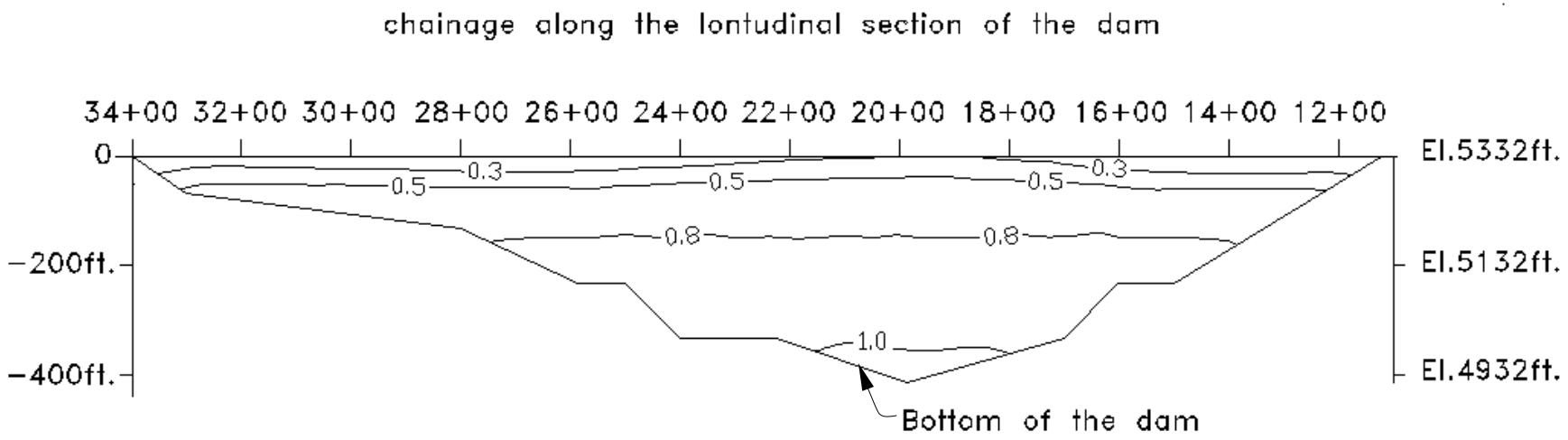

Figure 5-9: Contours of LI $_5$ on the longitudinal section of the dam

CHAPTER SIX

DISCUSSION OF RESULTS

6.1 New mechanism of Teton failure

A rigorous analysis has been performed to determine the stresses, q and p' and stress ratio q/p' in the dam. The contours of q/p' are shown in Figure 5-8 for a typical cross-valley section. The state based soil mechanics theory presented in Chapter 2 suggests that zones with stress ratio q/p' larger than 3 would indicate the presence of a vertical split or crack (Fig. 2-6). It can be seen that the majority of the soil elements have q/p' stress ratios significantly less than 3 indicating that they were intact (Fig. 5-8). However, there were two zones that have q/p' ratio larger than 3 (Fig. 5-8). They are from Sta. 13+00 to Sta.15+00 in right side and from Sta. 26+00 to Sta. 28+00 left side.

The results clearly show that at the end of construction the state of stress in the dam core had significantly reached into the crack surface (q/p'=3) region which is an indication of the existence of internal cracks at two locations, Sta.14 + 50 in the right abutment and Sta.26 + 50 in the left abutment. The cracks at Sta. 14+50 were 32 feet deep from top of the crest while they were only 10 feet deep at Sta.26+50 (see Fig. 5-8). The state based theory further suggests that contours of the q/p' ratio less than 3 would indicate the stable nature of the compacted soil, which is the case for soil elements at depth and particularly below 32 feet (Fig.5-8). Therefore, it is concluded that the failure of the Teton dam was initiated as a result of water flowing through the deepest open vertical crack on the right abutment near Sta. 14+50 during the first filling when the water level reached the bottom of the crack, which slowly eroded the crack into a large tunnel leading to the major breach hours later.

The zone-1 core was capped by a 3-foot layer of sand and gravel roadbed, which was subjected to continual vibration and compaction by vehicular traffic inhibiting cracks in the layer. Further, the material parameters of the granular bed, their packing, and the characteristics were different from zone-1 material to exhibit cracking. As a result, it was likely that the cracks below in the core zone apparently had not daylighted onto the roadbed and were not visible during first filling. However, numerous transverse cracks daylighted the roadbed in the left abutment soon after the dam breach, mostly near Sta. 26+50, where the q/p' ratio was close to or larger than 3 for shallow depths.

The contours of LI_5 (Fig. 5-9) independently confirm that only shallow depths to about 30 ft between Sta. 14+00 and Sta.+ 16+00 are prone for cracking. Because of the low plasticity (PI ~ 4), the liquidity index was very sensitive to placement water content and its influence on the performance of the soil core, under rapidly changing confining and shear stress conditions, particularly at the abutments. At the steep abutments, depth of the soil column decreases; consequently the soil elements were subjected to decreased confining stress. In effect, the stress states of the soil in the abutments were in the Hvorslev regime and were more stiff while those in the valley section of the dam were in or near the ductile (Cam clay) regime, which were more deformable. Again the changes in the deformability were further disrupted by the benches, which apparently caused significant differential deformations and increased shear stresses at some locations. These aspects were well reflected in the stress analysis.

In earth structures such as the Teton dam, fill materials are generally placed at or near the optimum water content to achieve a high density. The construction specification generally used the “optimum water content” as the reference point. At this state, the

material is partially saturated (80-85%), near the plastic limit (PL) (low liquidity index), has higher stiffness, constrained modulus, and strength. For this placement condition, the state of soil (3>q/p'> 1.1) remains in the Hvorslev regime of the stress-space (Fig. 6-2). However, if the placement water content is increased, the liquidity index will be increased. Consequently the material will become less stiff and more ductile. With increased confining stress or water content, the equivalent liquidity index would increase and consequently the state of soil can quickly migrate into the Cam-clay yield regime (1.1>q/p'>0). The soil would then deform with positive pore water pressure response. Because of the low plasticity index of the Teton core (Zone-1), small changes in water content played a significant role in altering its liquidity index and the mechanical properties including the potential for cracks/rupture and ductility.

6.2 Critique on past investigations

The concepts presented may also help explain some of the misgivings of previous investigations. Consider the states of soil element shown in Figure 6-1 (A_1, A_2, A_3, and A_4). At the placement condition, the state of soil would have been at point A_1 in Figure 6-2, which was in Hvorslev region. As the dam was built up, the confining stress would increase and the state of soil would move in the path $A_1A_2A_3A_4$ (Figure 6-2). The soil, which was in the key trench, would move to the Cam clay stable yielding region when it was wetted.

It is, therefore, concluded that the hydraulic fracture in the key trench ((Seed et al, 1976, Sherard, 1987) and its relevance to the failure of the dam is fundamentally flawed (See also Muhunthan and Schofield, 2000). Except for the shallow depths of 30

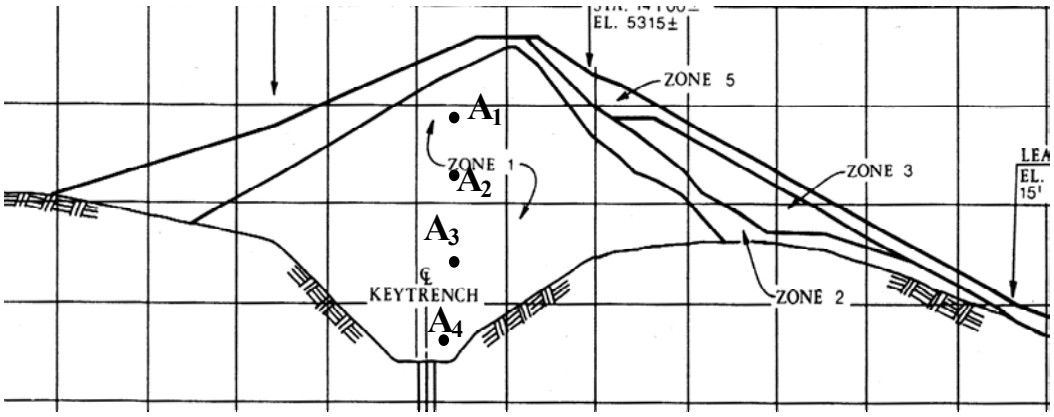

Figure 6-1: Cross section of the dam at the right abutment

to 35 feet in some location, the q/p' stress ratio is significantly lower than 3 (fracture level), which indicates that fracturing of the soil would be difficult with increasing depth (Fig.5-8). For hydraulic fracture to occur, the soil element must be subjected to seepage water, which can cause (a) physical wetting of the soil first and then (b) a corresponding hydraulic pressure in the soil. The physical wetting and saturation of the soil increases the liquidity index of the in-situ soil and consequently the soil element becomes more ductile and the material tighter and less permeable (Fig.2-11) (also the q/p' ratio drops off quickly, Fig.6-2 (a)). That is the stress-path moves significantly to the right to a more ductile and stable yield (Cam-clay) regime (Figure (6-2).

Some researchers (Leonard and Davidson, 1984) characterized the phenomenon of yield as "collapse on wetting", which is a misnomer considering that the stress path simply migrated from the stable Hvorslev regime to the stable ductile Cam-clay regime. On the second point, (b), the hydraulic pressure due to the water seepage would have a limited opposite effect of reducing the effective stress of the soil element. Any such reduction in effective stress due to the seepage pressure will be more than offset by

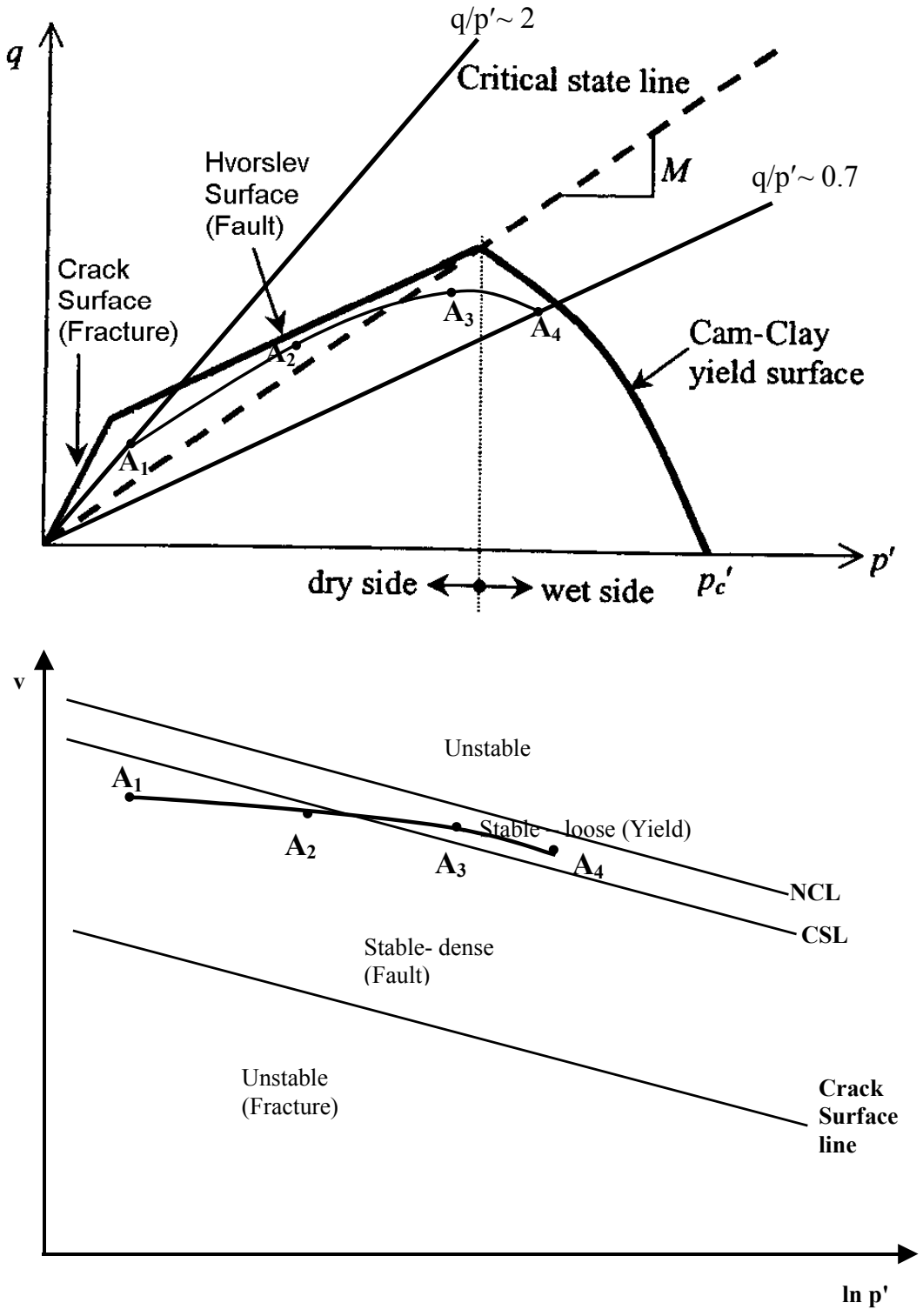

Figure 6-2: Stress path of soil state during the construction of the dam (Schematic)

changes in the mechanical properties (ductility) of the soil. The net effect is the movement of the stress-path of the soil element is to the right and towards the Cam-clay regime (Fig. 6-2). Therefore the notion of "hydraulic fracture" by water pressures equal to or less than the reservoir head, which could initiate a failure of the dam, has no scientific basis. In fact, to cause hydraulic fracture in the soil at the base of the dam (Cam clay state), one needs to apply a hydraulic head of about 800 ft. of water!

It is also concluded that the "wet seam" theory postulated during post-failure investigations (Leonards, 1987, Hilf, 1987) is fundamentally flawed. The majority of the core material on Zone-1 was placed at a negative liquidity index (0.25 – 0.50) or in the Hvorslev regime in the stress-space (Figs. 6-2, 2-11). When seasonal rains and snow condition interrupted the material placement during construction, some layers might have been placed at wetter than the average or near liquidity index of unity. When subjected to large stresses, such pockets of material would fall into the Cam clay ductile regime and deform like potter's clay, "wet-seams" or wet-pockets producing positive pore water pressure. This was the case for a few random pockets/layers of fill that were affected by the rain/snow when full stripping and replacement of such layers were not possible during the construction. Although such layers were of low strength and stiffness, they provide more impermeable mass relative to the surrounding material and would have had no adverse effect on the performance of the dam.

The original design specifications of Teton dam stipulated placement water content of optimum minus 1% to optimum for the core, which had only a small plastic index (PI<4). Based on our analysis, it is believed that this was the fundamental error in the design concept in leading to the demise of the dam. The placement water content

represented an initial liquidity index of zero or negative, which allowed considerable depth of the core to be prone to fracture (Fig. 6-2). Without compromising the compacted density, for this material an additional one to two percent water content would have provided adequate equivalent liquidity index of at least 0.5 or more for most of the placed fill. This would have kept the entire fill intact in the Hvorslev regime where the material would have been stiffer, stronger and water tighter except for the top 5 to 10 feet (freeboard regime). Therefore, it is evident that the lack of knowledge at that time of the combined effect of liquidity and confining stress in controlling the mechanical behavior of Zone 1 contributed in a major way to the Teton dam failure. For the design of earth-structures, the theory based on the "state based soil mechanics" provides a better understanding of the physical and mechanical behavior of a broad spectrum of soils including that of Teton dam, which are subjected to different loading conditions.

CHAPTER SEVEN

CONCLUSIONS AND RECOMMENDATIONS

7.1 Conclusions

A new theory is postulated for the failure of Teton dam based on the concepts of fundamental soil mechanics. Based on the investigation and the discussion, it is concluded that:

1. A transverse crack(s) or large opening(s) had developed in the core (Zone-1) to a maximum depth of 32 feet below the crest (top of the core) at the right abutment near Sta. 14+00. Also, the rigorous stress analysis further indicates that the stress state conducive to internal cracks existed in the core in both abutments in the upper portion of the dam at much shallower depths. When the reservoir level rose to the level of the deepest crack, water flowed freely, barreling downstream into the chimney drain (Zone 2), causing a spontaneous failure of the dam a few hours later.

2. The internal cracks might not have daylighted through the 3-ft thick granular roadbed, which was subjected to constant vehicular traffic and compaction. Also, the parameters that control the behavior of the core were different from those of the overlying roadbed granular fill.

3. The uniform clayey silt (CL-ML) that was used for the core of Teton dam fitted well into the CSSM model that was developed for other soils with different plasticity. Although the clayey silt had relatively high values for the liquid limit (LL~27) and plastic limit (PL~23), the plastic index was relatively small (PI~4 or less). Consequently the liquidity index was very sensitive to the initial placement

water content and its subsequent changes in mechanical properties due to varying confining stress. This phenomenon was a significant contributor to the cracking of the dam. Therefore, for clay-silt cores, it is more prudent to have the construction specification refer the "placement water content" with respect to the plastic limit (PL), than to the optimum water content.

4. A combination of material parameters such as the low plasticity of the core, the sensitivity of the liquidity index of the material to water content, its variation under the subsequent confining stress condition, and their influence on the constrained modulus played a key role in the cracking of the core. It appears that these aspects of fundamental soil mechanics and the phenomenon of cracking were not recognized in the original design of the dam.

5. The theoretical models based on "state based soil mechanics" used in this study provide a better scientific understanding of the influence of confining stresses and the changes of the mechanical behavior (stress-deformation) relating to the state of soil in the stress-space and physical properties such as liquidity index and water content.

7.2 Recommendations for further research

The state based concept proposed here is sound for the characterization of shear behavior of soils in the field. It must, however, be recognized that the critical state framework on which the concepts were developed here was based on properties of reconstituted evaluated soils in the laboratory.

Mechanical behavior of natural clays, however, has been found to differ from reconstituted soils in a number of important ways (Leroueil 1997; Leroueil and Vaughan 1990; Burland 1990; Mitchell 1993). These materials possess a significant degree of anisotropy developed over the geological period under the influence of both depositional environment and post-depositional processes. The shapes of the yield curves of most natural soft clays depend on the history of the depositional environment.

It has been observed experimentally by many researchers that the anisotropic stress history causes a rotation of yield surface and plastic potentials. These studies have shown that the initial yield surface of normally consolidated natural clays is oriented along a line close to the earth pressure at rest (K_0) (Mitchell 1970; Wong and Mitchell 1975, Tavenas and Leroueil 1977, 1980; Graham et al. 1983) and not along the isotropic axis as predicted by the classical critical state models. It is necessary to incorporate the influence of anisotropy into the constitutive models to model better the behavior of natural clays.

The shear behavior of most soils in the field is on the dilative side of the critical state. Therefore, the fracture and fault surfaces must be included as part of a constitutive model. In the analysis here, ABAQUS used two ellipses to capture the effects on the dilative side (Fig. 5-4). It can be improved by including a fracture surface so that those regions can be directly identified from the analysis.

The tensile fracture criterion was identified as in the vicinity of $p'/p_{crit} = 0.1$, as indicated in Figure 2-6. This position may need to be changed based on additional data. Perhaps a tensile strain criterion will provide a better fit to data for splitting in compression and spalling in extension (Schofield, 1980).

REFERENCES

ABAQUS : Finite element software package, (2003), Version 6.3-1, Habbitt, Karlsson and Sorrenson, Inc.

Atkinson, J.H., 1993. An introduction to the mechanics of soils and foundations, McGraw Hill, London.

Graham, J., Noonan, M.L., and Lew, K.V. 1983. Yield states and stress–strain relations in natural plastic clay. Canadian Geotechnical Journal, 20: 502–516.

Hilf, J.W, 1987, The wet seam and the Teton Dam Failure, Engineering Geology, 24, pp 265-278.

Houlsby, G.T and Wroth, C.P, 1991. The variation of shear modulus of a clay with pressure and overconsolidation ratio, Soils and Foundations, Japanese society of soil mechanics and foundation engineering, Vol. 31, No. 3, pp 138-143.

Independent Panel (IP), 1976. Report to U.S.Department of Interior and State of Idaho on Failure of Teton Dam, U.S. Government Printing Office, Washington, D.C.

Interior Review Group (IRG), 1980, Failure of Teton Dam-Final Report, USBR, Engineering and Research Centre, Denver.

Ladanyi, B., (1969). "Discussion of undrained strength characteristics of cohesionless soils," by H.B. Seed and K.L. Lee., Jour. Soil Mech. and Found. Div., ASCE, Vol. 95, No. 1, pp. 392-397.

Leonards, G.A. and Davidson, L.W., 1984. Reconsideration of failure initiating mechanisms for Teton Dam. Proc. Int. Conf. Case Histories in Geotechnical Engineering, St.Louis, Mo, May 7-11, Vol. III, pp. 1103-1113.

Leonards, G.A. (Ed), 1987. Special Issue on Dam Failures, Engineering Geology, 24,Nos 1-4.

Muhunthan, B and Schofield, 2000. Liquefaction and Dam Failures, GeoDenver-2000, Denver, Colorado.

Muhunthan, B. Chameau, J.L., and Masad, E. (1996) : "Fabric effects on the yield behavior of soils," Soils and Foundations, Vol. 36, No. 3, pp. 85-97.

Lee, S.W, Bolton, M.D, Mair, R.J, Soga, K. and Hagiwara, T., 2002. Modelling of sequential injections near tunnel linings, Soils and Foundations, The Japanese geotechinical society, Vol.42, No.6, pp.9-22.

Leroueil, S., and Vaughan, P.R. 1990. The general and congruent effects of structure in natural soils and weak rocks. Géotechnique, 40(3): 467–488.

Luis E. Vallejo, 1993. Shear stresses and the hydraulic fracturing of earth dam soils, Soils and Foundations, Japanese society of soil mechanics and foundation engineering, Vol. 33, No. 3, pp 14-27.

Mitchell, R. J., (1970) : "On the yielding and mechanical strength of Leda clays," *Canadian Geotechnical Journal*, Vol. 7, No. 3, pp. 297-312.

Olcott, D.L (2001). Energy dissipation and critical state strength of sand, MSc Thesis , Washington State University.

Penman, A.D.M, 1987. Teton Investigation- A review of Existing Findings, Engineering Geology, 24, pp 221-237.

Pillai, V.S., and Muhunthan, B, 2001. A Review of the initial static shear (K) and confining stress (K) on failure mechanisms and earthquake liquefaction of soils, Proc. 4th Int. Conf. On Recent Advances in Geotechnical Earthquake Engineering and Soil Dynamics. San Diego, CA, March 26-31, paper # 1.51.

Pillai, V. S., and Muhunthan, B. (2002). Discussion of An investigation of the effect of soil state on the capacity of driven piles in sands, by Klotz, E.U. and Coop, M.R., Geotechnique Vol. 52(8), 620-621.

Raveendra, M. (2000). Some aspects of energy dissipation during shear deformation of sand. MSc Thesis, Washington State University.

Roscoe, K. H., Schofield, A. N., and Wroth, C.P. (1958). "On the yielding of soils." Géotechnique, 8(1), pp. 22-53

Roscoe, K. H. and Burland, J. B. (1968). On the generalized stress-strain behavior of wet clays. *Engineering Plasticity*, University Press, Cambridge, 535-609.

Roscoe, K.H., Schofield, A.N., and Thurairajah, A , 1963. Yielding of clays in states wetter than critical. Geotechnique, 13 (2), 211-240.

Schofield, A.N. 1966. "Original teaching on Cam-clay", Lecture notes, Cambridge University Engineering Department.

Schofield, A.N. 1980. Cambridge geotechnical centrifuge operations, 20th Rankine Lecture, Geotechnique, 30(3), pp.227-268.

Schofield, A.N (1980), "Some laboratory tests of Teton dam core soil illustrating well fracture, internal erosion, void migration, and interaction between fractures and filters", A report to the U.S. Department of the interior water and power resources service.

Schofield, A. N., (1998). " Mohr-Coulomb Error Correction," Ground Engineering, August 1998.

Schofield, A. N., and Togrol, E., (1966). "Critical states of soil." Bulletin of the Technical University of Istanbul, No. 19, pp. 39-56.

Schofield A.N. and Wroth, P, 1968. Critical State Soil Mechanics, McGraw-Hill.

Seed, H.B., Leps, T.M.,Duncan, J.M.,and Bieber, R.E., 1976. "Hydraulic fracturing and its possible role in the Teton dam failure" Appendix D of Report to U.S. Department of the Interior and State of Idaho on Failure of Teton Dam by Independent Panel to Review Cause of Teton Dam Failure, pp.D1-D39.

Seed, R.B and Duncan, J.M, 1986, FE analysis: Compaction-Induced stresses and deformations, Journal of Geotechnical Engineering, Vol. 112, No. 1, pp 23-43
Sherard, J.L. 1987. Lessons from the Teton Dam Failure, Engineering Geology, 24, pp 239-256.

Tavenas, F. and Leroueil, S. (1977): "Effect of stresses and time on yielding of clays," Proceedings of the 9th International Conference on Soil. Mechanics and Foundation Engineering, Tokyo, Vol. 1, pp. 319-326

Wong, P.K.K. and Mitchell, R.J. (1975) : "Yielding and plastic flow of sensitive cemented clay," *Geotechnique*, Vol. 25, No.4, pp. 763-782

Wood, D. M., (1990). "Soil Behavior and Critical State Soil Mechanics", Cambridge Press, New York, NY.